TERNARY FISSION STUDIES OF ^{235}U

TERNARY FISSION STUDIES OF ^{235}U

By

GERHARD (GARY) KUGLER, B.Sc.

A Thesis

Submitted to the School of Graduate Studies

in Partial Fulfilment of the Requirements

for the Degree

Doctor of Philosophy

McMaster University

October 1970

DOCTOR OF PHILOSOPHY (1970) (Physics)

McMASTER UNIVERSITY
Hamilton, Ontario.

TITLE: Ternary Fission Studies of ^{235}U

AUTHOR: Gerhard (Gary) Kugler, B.Sc. (McMaster University)

SUPERVISOR: Dr. W. B. Clarke

NUMBER OF PAGES: ix, 115

SCOPE AND CONTENTS:

Part I describes experiments carried out to search for possible products of ternary fission of ^{235}U. Inert gases extracted from neutron-irradiated ^{235}U were analyzed mass-spectrometrically for the presence of stable and radioactive neon and argon isotopes. No evidence for fission product neon or argon was found. Upper limits obtained for the yields are orders of magnitude lower than those suggested by some other studies.

Part II describes measurements of relative yields and energy distributions of ^{3}H, ^{3}He, and ^{4}He produced in fission of ^{235}U. A short-range (<8 Mev) component in ^{4}He, not previously established, has been detected in this work. The upper limit obtained for direct formation of ^{3}He is lower by two to four orders of magnitude than the frequency of formation of ^{3}He found in studies of other fissile nuclides.

ACKNOWLEDGEMENT

My sincere appreciation for his guidance throughout the course of this work is extended to Dr. W. B. Clarke. He provided an environment which always encouraged an original approach, and for which I am grateful. I am also indebted to Dr. T. J. Kennett and Dr. R. H. Tomlinson for helpful discussions.

This work was made possible through fellowships from the Canadian Kodak Co., the Ontario Government, and the National Research Council of Canada.

TABLE OF CONTENTS

LIST OF TABLES

LIST OF ILLUSTRATIONS

PART I

SEARCH FOR NEON AND ARGON ISOTOPES AS POSSIBLE PRODUCTS OF TERNARY FISSION OF ^{235}U

I

INTRODUCTION

A. HISTORICAL NOTES

For the last three decades nuclear fission has attracted the attention of scientists throughout the world and it appears that we are still only beginning to understand this highly interesting and complex phenomenon. Many practical applications of the energy and radioactive isotopes produced in fission have been realized and undoubtedly numerous others wait to be exploited. Aside from its practical uses however the fission process has made possible the study of nuclear matter under such physical conditions as can not readily be obtained by any other process.

The efforts which followed its discovery by Hahn and Strassmann in 1939 (1) soon delineated some of the important features of fission. The basically asymmetric mass division and the release of about 200 Mev of energy in the fission act were realized almost immediately. Also, the emission of two to three neutrons, the greater fissionability of even-even nuclei as compared to other nucleon assemblies, and the fact that fission can give rise to

several hundred different products were apparent very shortly after the results of the early experiments were made known. The first attempt to explain these features theoretically was made by Bohr and Wheeler (2) based on the analogy of an excited nucleus to a charged liquid drop. Bohr and Wheeler's theory accounted for some features quite well but could not explain the asymmetric nature of the mass-yield curve for fission fragments, a problem which still awaits an adequate theory. In fact it was perhaps due to the shortcoming of the Liquid Drop Model on this count that Wheeler (3) first suggested ternary fission, a splitting of the nucleus into three parts, as a possible explanation for the asymmetric mass distribution. The type of mass split envisioned by Wheeler was one in which two products would have a mass of about 100 and one product a mass of about 40 amu.

The possibility that such a division in mass may occur was soon investigated by Present and Knipp (4). Using the Liquid Drop Model they showed that ternary fission is in fact energetically more favourable than binary fission, since about 20 Mev more energy would be liberated when a heavy nucleus divides into three roughly equal parts, as compared to the energy released when two fragments are formed. They also showed that the nuclear surface could be expected to deform in such a way that three equal collinear

fragments would result. Despite the highly exothermic nature of ternary fission Present (5) argued that since the path traversed on the potential energy surface in forming three equal fragments is not that of steepest descent this process would be less probable than binary fission. A search for ternary fission products was initiated during the Manhattan project. Metcalf, Seiler, Steinberg, and Winsberg (6) conducted radiochemical analyses of the fission products of ^{235}U in the region from 35 to 59 amu on isotopes of S, Cl, Ca, Sc, and Fe, but failed to detect any with a yield greater than about 10^{-4} per cent. The conclusion which followed was that ternary fission was indeed a very improbable mode of fission and could not be responsible for general features of fission yield systematics.

Although a search for ternary fission products did not appear to offer any practical usefulness it was realized by those interested in fission that the study of ternary fission could perhaps shed some light onto some of the fundamental problems of fission. In particular, ternary fission would afford a unique opportunity of studying nuclear matter under extreme conditions of deformation and perhaps show more clearly the role which underlying shell structure plays in fission. Ternary fission, especially of the type where a light charged particle such as an alpha particle is emitted (discussed in Part II of this thesis), is now

being studied in several laboratories using the techniques of radiochemistry, nuclear emulsions and other track detectors, coincidence circuits employing solid state detectors and multi-parameter data recording, and mass spectrometry.

Following early radiochemical work which met with negative results in the search for evidence of ternary fission, Alvarez (7) first observed triple fission into two heavy particles and one light particle, an alpha particle. This mode of fission has since then been observed by numerous research groups and is now well established. Ternary fission in which the lightest fragment has a mass in the region spanning 20 to 60 amu has been the subject of some recent work. Its existence has been verified by some experiments but has been ruled out or at least deemed extremely improbable by others. Part I of this thesis describes a search for possible products of this ternary fission process.

B. EVIDENCE FOR AND AGAINST TERNARY FISSION

Recent work in high energy fission shows that ternary fission may be a significant mode of decay for very highly excited compound nuclei with fissionability parameters $Z^2/A \gtrsim 40$. Such situations may be realized by bombarding targets of Pb, Th, or U with ions such as Ne or Ar of several

hundred Mev of energy. Fleischer et al. (8) using track detection methods have reported a value of TF/BF (Ternary Fission Yield/Binary Fission Yield) of 1/30 when ^{232}Th is bombarded with 400 Mev Ar ions. A value for TF/BF of $(1.3 \pm 0.3) \times 10^{-3}$ was reported by Karamyan et al. (9) for the case $^{238}U + ^{40}Ar$ (310 Mev) using coincidence techniques. Some other cases showed lower TF/BF values. These results appeared to show some definite dependence of the ratio TF/BF on the excitation energy and the value Z^2/A of the compound nucleus in question. Radiochemical evidence for ternary fission has been obtained by Iyer and Cobble (10, 11) who detected ^{24}Na, ^{28}Mg, ^{31}Si, ^{38}S, ^{47}Ca, ^{56}Mn, and ^{66}Ni for the case ^{238}U + He (20 - 120 Mev). They also noted the absence of possible complimentary binary fission products, such as ^{183}Ta, ^{184}Ta, ^{199}Au, ^{209}Pb, and ^{212}Pb, and therefore ascribed the low mass products to ternary fission. The excitation functions obtained for some of the light fragments showed a rapid decrease in the cross sections at lower energies. Iyer and Cobble concluded from an extrapolation of the excitation functions to low energies that it would be highly unlikely that products such as ^{28}Mg could be observed in thermal neutron or spontaneous fission.

Observations of triple fission events at low energies have nevertheless been reported and some recent experiments especially seem to point toward the occurrence

of such events. The first reported positive evidence for thermal neutron ternary fission of ^{235}U came from the observation of three prong fission fragment tracks on nuclear emulsions. Hyde (12) gives a short review and pertinent references to some of these experiments. Due to the poor statistics inherent in such experiments the TF/BF values reported range from 1/5,000 (13) to <1/250,000 (14). Rosen and Hudson (15) have used a triple coincidence circuit to detect the three pulses produced by three ions of comparable mass in an ionization chamber which was divided into three parts. They observed a ratio TF/BF of $(6.7 \pm 3.0) \times 10^{-6}$ in the case of ^{235}U, and this value would be a lower limit only since they discriminated against fragments with energy <40 Mev. The most extensive studies on low energy ternary fission have been made by Muga and co-workers (16, 17, 18, 19, 20). This group has made triple coincidence measurements using solid state detectors placed at angles of 120° to each other, and around the fission source, on thermal neutron fission of ^{233}U, ^{235}U, ^{239}Pu, ^{241}Pu, and spontaneous fission of ^{252}Cf. Values for TF/BF of $(15 \pm 2) \times 10^{-6}$, $(7 \pm 2) \times 10^{-6}$, $(4 \pm 1) \times 10^{-6}$, $(3 \pm 1) \times 10^{-6}$, and 1.1×10^{-6} were found for the above cases, respectively. Because of the fixed angular arrangement of the detectors these values are again lower limits. In the case of ^{235}U

fission these workers claim to have found a peak in the mass distribution for the lightest fragment at ~38 amu and an extension of the curve to masses as low as ~20 amu.

Some radiochemical studies have been carried out in attempts to verify Muga's measurements. Stoenner and Hillman (21) have looked for the radioactive argon isotopes and Prestwood and Bayhurst (22) for ^{7}Be, ^{28}Mg, ^{38}S, ^{48}Sc, ^{51}Cr, $^{54,56}Mn$, ^{59}Fe, and $^{56,57,58,60}Co$ as possible products of ternary fission of ^{235}U but have observed yields or set upper limits to these from one to several orders of magnitude lower than Muga's measurements would suggest. The apparent contradiction in evidence from instrumental results to that of the radiochemical findings might possibly be resolved, as suggested by Muga, if the mass distribution in question were either extremely narrow, and therefore the light mass product has as yet escaped detection, or else these products are formed as stable nuclides.

Further positive evidence for ternary fission at low energy has been suggested by an entirely different type of study. Measurements of the isotopic composition of argon found in uranium bearing minerals by several groups (23, 24, 25, 26) have indicated the presence of anomalous components of ^{38}Ar and ^{40}Ar. The origin of these isotopes has usually been ascribed to nuclear reactions induced by either α particles or neutrons on targets of Cl and K present in

the rocks. One group (25) has however concluded that the excess ^{38}Ar must be due to either spontaneous ternary fission or extreme asymmetric fission. In another study (26) the constant correlation of the ^{38}Ar and ^{40}Ar excesses and their apparent independence of the widely varying chemical composition of the minerals led to the conclusion that ^{40}Ar also is a product of spontaneous fission of ^{238}U.

Both positive and negative evidence for the existence of ternary fission cited in this introduction have in part prompted the present search for the stable (and some unstable) isotopes of neon and argon produced in ternary fission of ^{235}U. The approach was to purify samples of uranium oxide enriched in ^{235}U, irradiate these in the McMaster reactor, extract the inert gas fission products, and analyze these for total content and isotopic composition using a mass spectrometer.

II

EXPERIMENTAL

A. SAMPLE PREPARATION

(i) Purification of uranium oxide samples.

The evidence described in the introduction indicates clearly that ternary fission products are formed with extremely low yields at most, and hence high purity fissile samples and ultra-high sensitivity methods for the detection of possible ternary fission products are required. Since the products searched for in this work were isotopes of the inert gases neon and argon it was imperative to purify the uranium oxide samples prior to irradiation. Attention was focussed on atmospheric neon and argon as well as possible impurities of F, Mg, Cl, K, and Ca, which could produce some isotopes of neon and argon under neutron irradiation. The major reactions involved are:

$$^{19}F(n,\gamma)^{20}F \xrightarrow{\beta^-} {}^{20}Ne$$

$$^{24}Mg(n,\alpha)^{21}Ne$$

$$^{25}Mg(n,\alpha)^{22}Ne$$

$$^{37}Cl(n,\gamma)^{38}Cl \xrightarrow{\beta^-} {}^{38}Ar$$

$$^{39}K(n,p)^{39}Ar$$

$$^{40}Ca(n,\alpha)^{37}Ar$$

The method chosen for purifying uranium oxide samples of these volatile components was to heat in high vacuum for prolonged periods of time. An irradiated sample of U_3O_8 enriched to 93.18% in ^{235}U used as a test sample showed that >99.8% of the fission product Kr and Xe was released after the sample had been heated at 1400°C for two hours. It was therefore decided that a three hour heating of the U_3O_8 samples at 1500°C should prove adequate in completely outgassing the samples of any atmospheric and radiogenic neon and argon. It was also expected that this process would decrease the content of volatile compounds of F, Mg, Cl, K, and Ca. Later measurements appeared to confirm this, or else these elements were present originally in very small amounts. In the case of Cl, as determined from measurements of the ^{38}Ar produced, the concentration in the samples after outgassing was at most a few parts per billion.

Heating of the uranium oxide was accomplished by means of a vacuum induction furnace, shown in Fig. I-1.

FIG. I – 1 . VACUUM INDUCTION FURNACE .

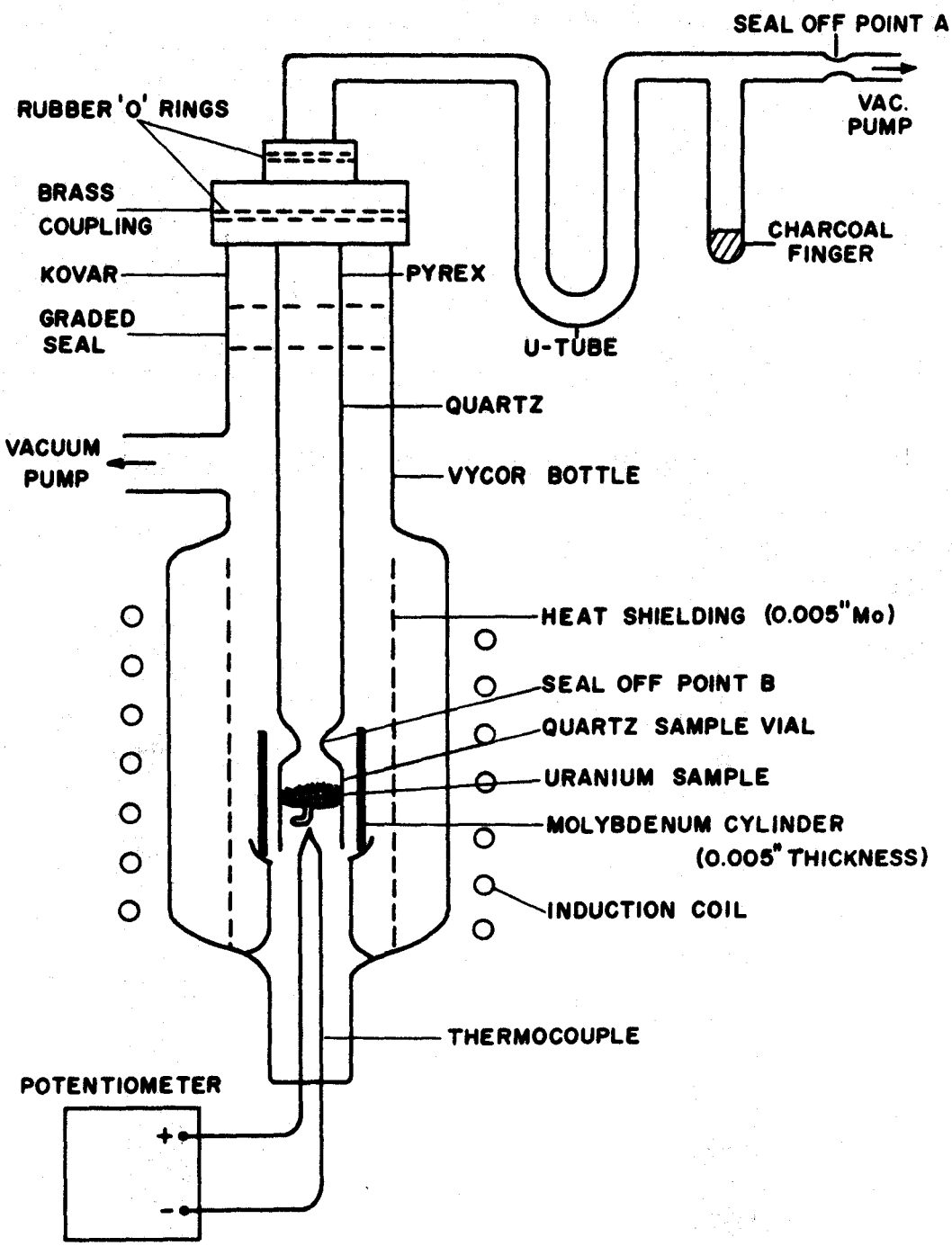

The sample was heated by radiation from a molybdenum cylinder, which in turn was heated by high frequency induction. Temperatures were measured with a tungsten 5% - tungsten 26% rhodium thermocouple. The procedure was as follows:

(a) Samples of U_3O_8 enriched in ^{235}U (1-9 mg) were placed inside the quartz sample vial.

(b) The sample vial and Vycor bottle were pumped down to a pressure of ~5 X 10^{-9} and ~10^{-5} torr, respectively.

(c) The sample was heated to 1500°C and held there for one hour.

(d) Gases evolved during heating were pumped away over a period of several hours.

(e) Steps (c) and (d) were repeated a total of three times.

(f) The sample system was sealed at point A, with the U-tube and charcoal finger at liquid nitrogen temperature.

(g) The sample tube was withdrawn from the Vycor bottle and the vial sealed off at point B (U-tube and charcoal finger still at liquid nitrogen temperature).

(ii) Irradiation details.

After purification the sample vials were wrapped

with Al foil (for heat dissipation) and sealed in standard Al cans for irradiation in the McMaster reactor. Several series of samples were prepared, irradiated, and analyzed, and each series indicated improvements in the experimental procedures for subsequent samples. Irradiation details for samples from which final results were obtained are given in Table I-1. An empty quartz vial was irradiated along with each sample to serve as a blank indicator.

Table I-1

Sample Details

Sample	Composition	Weight	Irradiation period *	Cooling period
A	U_3O_8 (93.18% ^{235}U)	9.0 ± 0.1 mg	3 months (low flux)	3 months
B	U_3O_8 (93.18% ^{235}U)	1.0 ± 0.1 mg	3 months (high flux)	2 months
C	U_3O_8 (93.18% ^{235}U)	1.0 ± 0.1 mg	3 months (high flux)	2 months

*Thermal neutron flux in the McMaster reactor is ~1.5 X 10^{13} neutrons/cm^2/sec.

The number of fissions incurred in the samples was determined from measurements of the amounts of ^{134}Xe extracted after irradiation and from the known fission yield of ^{134}Xe (a value of 8.06% was used (27)).

(iii) Extraction of fission product inert gases.

The fragments produced in fission recoil into the crystal lattice of the uranium oxide and are retained there quite firmly. Any inert gases so produced can be liberated by heating the samples at elevated temperatures ($\gtrsim$1000°C). The method used was essentially the same as that for purification of the samples, with only break-seal tubes and flasks added. The modified system is shown in Fig. I-2. Particular care was exercised during the extraction process since the samples containing the fission products were quite radioactive. Adequate shielding against β and γ radiation was provided by a 2 1/2" thick lead wall set up around the extraction system. The system was constructed of Pyrex and was built into a fume-hood in order to contain any volatile fission products which might be accidentally released during heating.

After a two or three month cooling period a vial containing the irradiated uranium oxide was sealed on to the extraction system at point A. The system was then

FIG. I-2. EXTRACTION SYSTEM.

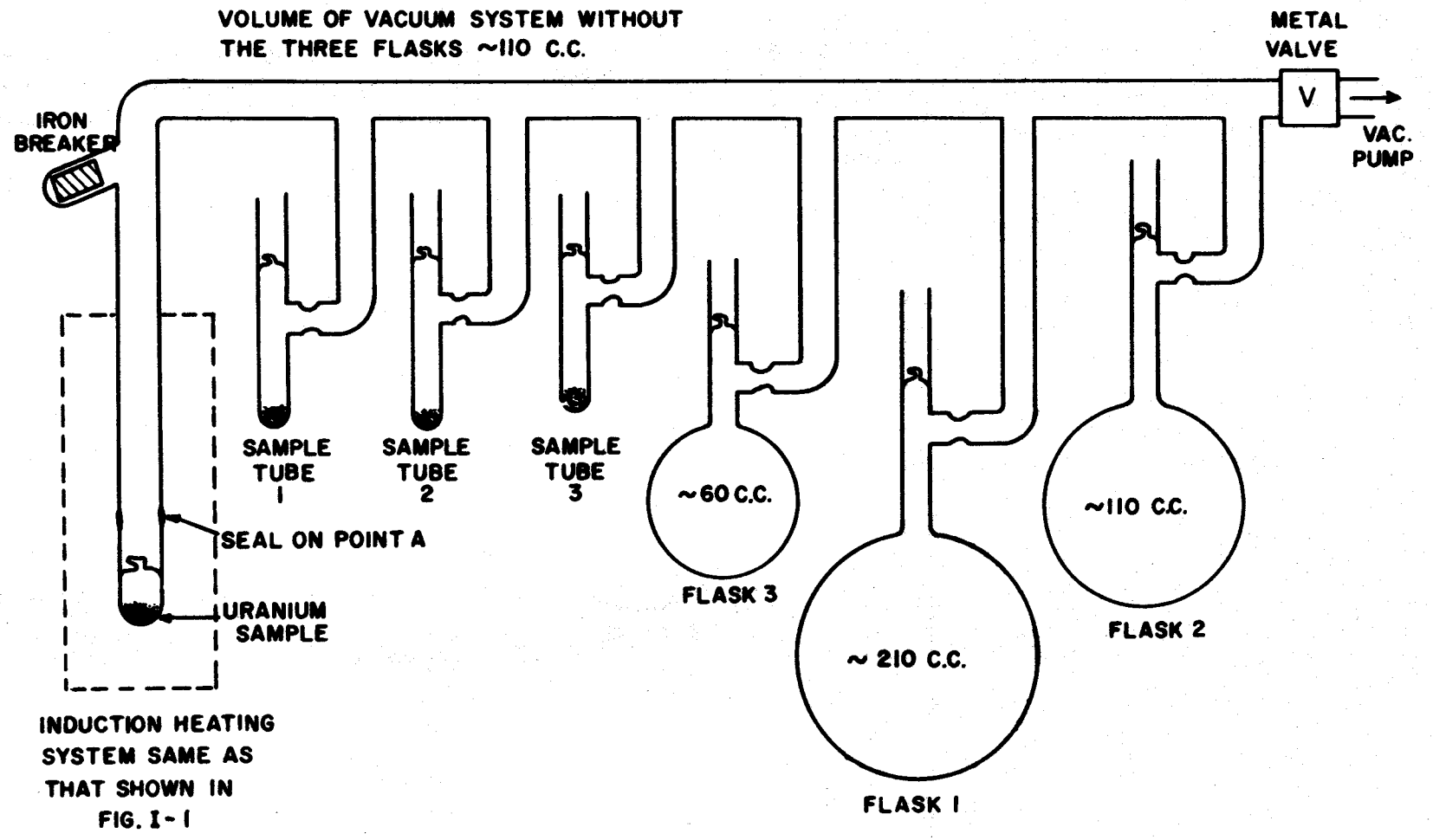

pumped down to a pressure of ~10^{-9} torr. This required heating the whole vacuum system at temperatures of ~300°C for one day and subsequent pumping at room temperature for another day. For this purpose an oven constructed of 1" Marinite board and using resistance heating elements was built around the vacuum system. When the required high vacuum was obtained, valve V was closed and the break seal of the sample vial broken with an iron slug. The sample was then heated for one hour at each of three different temperature plateaus and the gases evolved at each level were collected separately. Ar, Kr, and Xe were condensed in sample tubes containing activated charcoal held at liquid nitrogen temperature, and Ne was allowed to expand into the flasks. The collection efficiency for Ar, Kr, and Xe was essentially 100%, whereas the efficiency for Ne was determined by the ratio of the volume of a particular flask to the total volume of the isolated vacuum system. With the approximate volumes indicated in Fig. I-2 it can be seen that at each temperature plateau a 35-40% collection efficiency was obtained for neon (the flasks were sealed off in the order in which they are numbered in Fig. I-2).

For one of the early test samples the fission products present in the sample vial in the gas phase at room temperature were collected. This fraction served as

a check on possible diffusion loss, and hence possible fractionation of the inert gases, during irradiation. Only negligible amounts (<1% of total) of fission Kr and Xe were found in this fraction.

B. MASS SPECTROMETRY

(i) The mass spectrometer.

The mass spectrometer, see Fig. I-3, was a 10" radius first-order direction-focussing instrument. With source and collector slit widths of 0.1 and 0.3 mm, respectively, a resolving power of 620 was easily achieved. The ion source was a conventional electron impact type, and ion detection was accomplished with an electron multiplier (gain $\sim 10^5$) followed by a vibrating reed electrometer, appropriate amplifiers, and chart recorder. The ultra high sensitivity of this instrument for inert gases enabled detection of about 10^6 atoms of Ar, but for isotope ratio measurements with a precision of one or two per cent sample sizes of 10^8 atoms or greater were required.

(ii) Background and memory effects.

A background of hydrocarbons is found at almost all mass positions, but the excellent resolution of the

FIG. I-3. MASS SPECTROMETER AND SAMPLE SYSTEM.

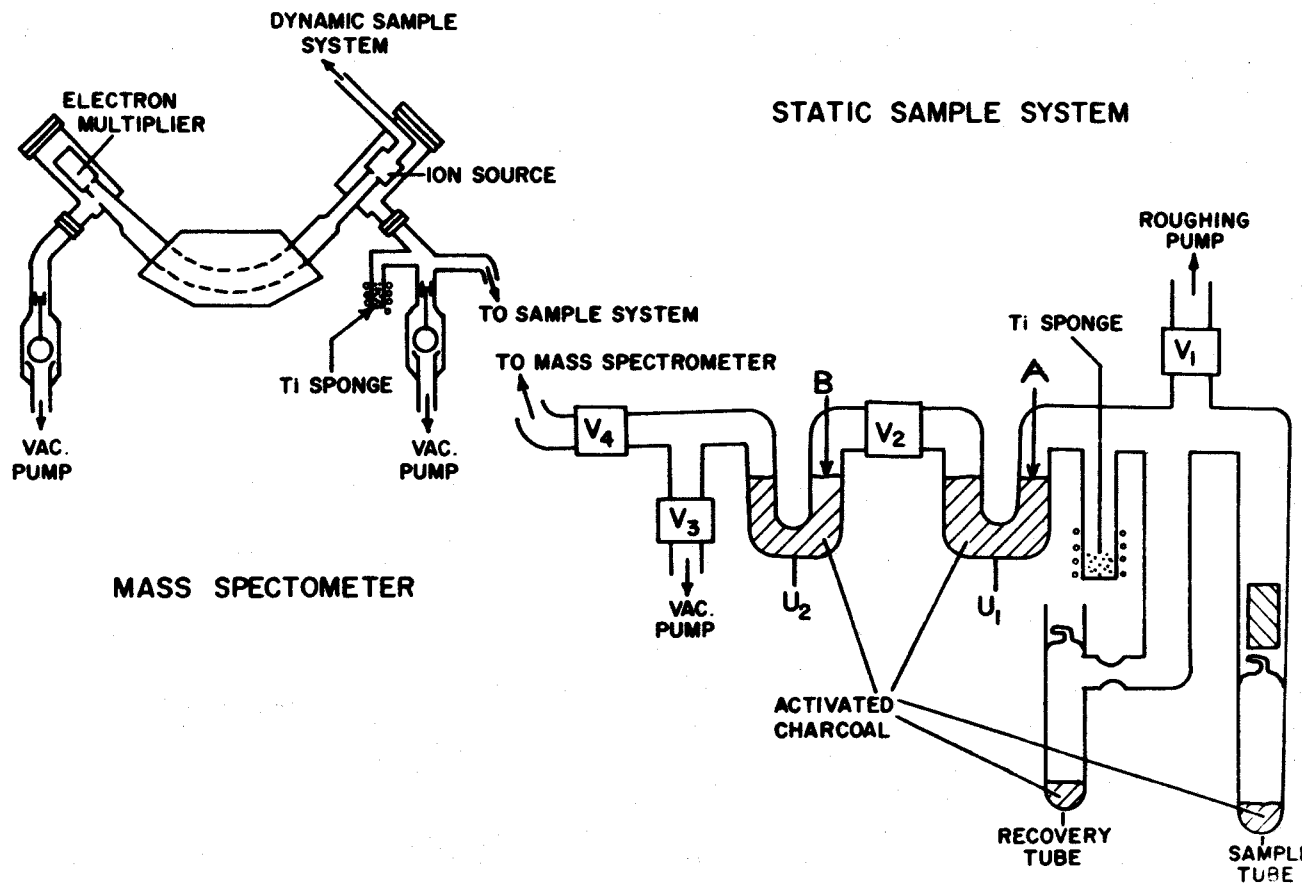

instrument can in most cases separate these from isobaric inert gas isotopes.

In the case of neon, a background of CO_2^{++} can enhance the peak of Ne^{22} and corrections are usually necessary. Free hydrogen in the mass spectrometer will enable the formation of inert gas hydrides. $^{20}Ne^{1}H$, in particular, may contribute appreciably to the ^{21}Ne peak.

A background of HCl and Cl must be considered when making isotope ratio measurements on small samples of argon. $^{1}H^{35}Cl$, ^{37}Cl, and $^{1}H^{37}Cl$ can not be resolved from ^{36}Ar, ^{37}Ar, and ^{38}Ar, respectively, and it is therefore desirable to reduce this background as much as possible. A method which can practically eliminate all traces of HCl and Cl is to heat the source assembly by electron bombardment. By operating the filament at an emission current of ~20 ma, while applying ~500 V between case and filament, for a period of one or two days, the HCl and Cl can be reduced considerably. Reductions of a factor of 100 from average background levels have been achieved. The low background so obtained is however only temporary. A gradual buildup over a period of weeks has always been observed.

Memory effects for ^{36}Ar have been noted in this instrument. The effect is due to remnants of samples highly enriched in ^{36}Ar which were analyzed at some earlier time.

Flushing the mass spectrometer with nitrogen at pressures of 10^{-6} to 10^{-5} torr for periods of several days reduced ^{36}Ar memory to tolerable levels.

Another type of background in argon analyses can be the interference of $^{84}Kr^{++}$ with $^{42}Ar^{+}$. It is therefore necessary to prevent any Kr from being introduced into the mass spectrometer simultaneously with the Ar samples.

(iii) Separation of neon and argon from krypton and xenon.

Krypton and xenon are formed with yields of several per cent in the fission of ^{235}U and ternary fission yields are expected to be smaller by a factor of $\sim 10^{4}$. Failure to separate any neon and argon from krypton and xenon before admission into the mass spectrometer would cause severe peak height depression when the analysis is performed by the static method. A second reason for this separation is the $^{84}Kr^{++}$ problem mentioned above.

Neon was separated from argon, krypton, and xenon during the original extraction process and no further separation was required. Argon was separated from krypton and xenon on the static inlet system shown in Fig. I-3. The procedure was as follows:

(a) The inlet system was pumped down to a pressure of 10^{-9} to 10^{-8} torr.

(b) V_1 and V_2 were closed, break seal of sample tube broken, and sample purified with the Ti getter.

(c) LN (liquid nitrogen) was placed on sample tube and Ar, Kr, and Xe recondensed. Timing with a stop-watch commenced.

(d) 14:00 min, LN was placed on U_1.

(e) 15:00 min, LN was removed from sample tube (Ar, Kr, and Xe allowed to condense at point A of U_1).

(f) 19:00 min, V_3 and V_4 were closed, LN placed on U_2.

(g) 20:00 min, V_2 was opened, LN removed from U_1 (gases diffusing through U_1 condensed at point B of U_2).

(h) 20:45 min, dry ice bath was placed on U_1 (at this temperature Ar diffuses through a charcoal column quite readily, Kr flow is retarded, and Xe is practically completely retained).

(i) 27:00 min, V_2 was closed.

(j) 28:00 min, V_4 was opened, and LN removed from U_2.

(k) 28:45 min, dry ice bath was placed on U_2.

(l) 35:00 min, V_4 was closed.

After step (l) analysis of the Ar isotopes was begun.

The efficiency of the separation will depend on the times, the diameter of the charcoal columns, and the type of charcoal used. Tests made on synthetic mixtures of Ar, Kr, and Xe showed that the gas fraction admitted into the mass spectrometer after the two stage separation contained

$74 \pm 3\%$ of Ar, $\lesssim 10^{-2}\%$ of Kr, and $\lesssim 5 \times 10^{-4}\%$ of Xe originally present. The Kr and Xe remaining in the inlet system were subsequently condensed in the recovery tube and later used to determine the number of fissions in the sample.

(iv) Peak height comparison method for the determination of sample size.

Absolute measurements of sample size are usually made by means of isotope dilution. In the present work this was however not suitable since it was necessary to measure the relative abundances of all isotopes of neon and argon. Therefore a peak height comparison method was used. Samples of known size were run immediately after the unknown samples and the relative peak heights of identical isotopes in the two samples provided a measure of the volumes of unknown samples. Care was taken to reproduce closely the conditions under which the two samples were analyzed. Also, the response of the mass spectrometer with respect to sample size had to be established. For small samples the response is expected to be linear, since the ion current is directly proportional to the partial pressure of the gas being analyzed. For large samples however peak height depression may occur, and therefore a check on instrument linearity was carried out.

A simple method to determine the mass spectrometer response, using only one sample, is as follows. The sample is allowed to expand throughout the inlet system (between V_1 and V_4; V_3 closed, in Fig. I-3). A fraction is isolated by closing V_2, admitted into the instrument, and its peak height measured. The fraction remaining between V_1 and V_2 is again expanded throughout the system, a second fraction isolated with V_2, and its peak height measured. Repeating this process several times permits a check on the response function over several orders of magnitude (the isolated fraction is preferably >1/2). If the response is linear the following relation should be satisfied:

$$\log Y_n = [\log (1-k)][n-1] + \log ka$$

where:

Y_n = peak height of the n^{th} fraction

k = constant fraction

n = fraction number

a = initial sample size

A plot of log Y_n vs. (n-1) should therefore yield a straight line. The response curve for a sample of argon, shown in Fig. I-4, indicates a linear relation over the region examined. All samples analyzed were well within this region. Accurately calibrated spikes of ^{36}Ar and atmospheric Ne were

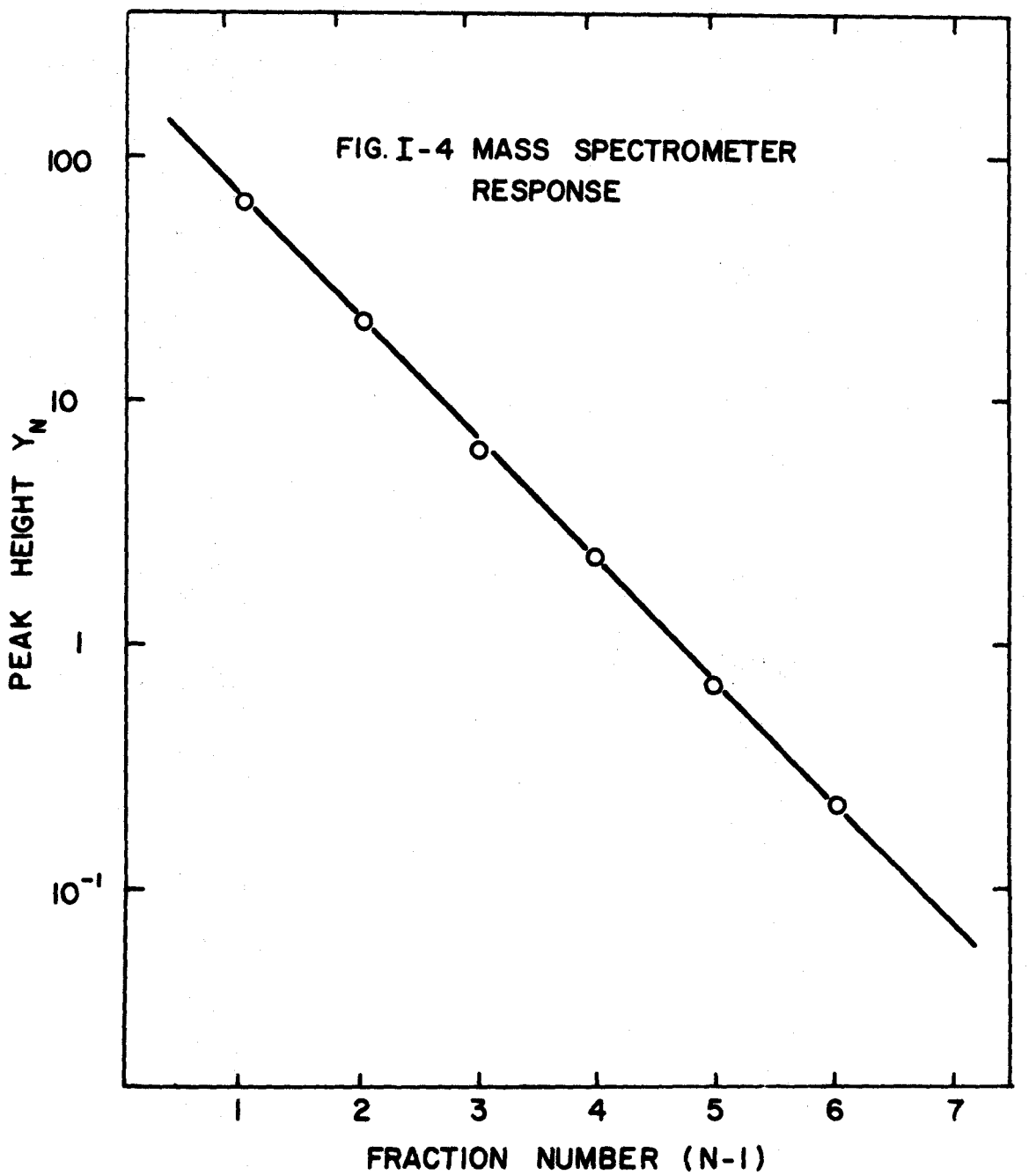
FIG. I-4 MASS SPECTROMETER RESPONSE
100
10
1
10^{-1}
PEAK HEIGHT Y_N
1
2
3
4
5
6
7
FRACTION NUMBER (N-1)

used as standards for the argon and neon measurements, respectively.

The peak height comparison method was also used to determine the ^{134}Xe contents. Measurements were made using the flow method of sample introduction. Calibrated spikes of atmospheric Xe and Kr in the ratio Xe/Kr = 7/1 were used for comparison.

(v) Sources of error.

(a) Measurement error.

Errors in measurement of peak heights are caused predominantly by statistical fluctuations in the ion currents. In most cases eight or more double scans of the mass spectra were taken and the probable errors of the isotope ratios due to measurement alone are about $\pm$1% (for $^{21}Ne/^{20}Ne$ this estimate is $\pm$2%).

(b) Fluctuations in memory and background.

Corrections to memory effects were made by extrapolating all measured isotope ratios back to the time of sample introduction, when the effects were negligible. Background effects, such as HCl and CO_2^{++}, were determined from measurements of the isotope ratios on samples of known composition. Atmospheric neon and

argon, with Eberhardt's (28) and Nier's (29) values, respectively, for isotopic abundances, were used as standards.

Despite these corrections small fluctuations between runs introduced an error in the measured isotope ratios. A probable error of 2% has been estimated for most cases. Due to the $^{20}Ne^{1}H$ problem and extremely small sample size errors for ^{21}Ne determinations were ± 4 %.

(c) Mass discrimination.

Mass discrimination effects can be caused during sample introduction (flow method only), in the ion source, and at the electron multiplier. These effects are however small by comparison. Moreover they were completely determined from measurements of the atmospheric standards.

(d) Calibration errors.

Errors in the calibrated spikes used in peak height comparison will introduce an uncertainty in measurements of absolute abundances. Added to this must be the effect of errors in separation and collection efficiencies for argon and neon, respectively. Slight non-linearities in mass spectrometer response will also contribute to this uncertainty. An estimate of the probable error in absolute abundances from all sources is ± 7 %.

III

RESULTS

A. NEON MEASUREMENTS

Neon was extracted from samples B and C (see Table I-1). Results of measurements of the isotope ratios and ^{20}Ne and ^{134}Xe contents are given in Table I-2.

The inert gases were extracted in three separate temperature fractions in an attempt to optimize the ratio of possible fission components to atmospheric components. It was also reasoned that any fission Ne and Ar would exhibit some correlation with fission Xe in the different temperature fractions. An uncertainty of $\pm 50°C$ was estimated for the temperature. This resulted from the variable positioning of the sample vial in the induction furnace.

In Table I-2 the deviation from atmospheric composition is expressed by "δ" values, where

$$\delta^{x} = \frac{(^{x}Ne/^{20}Ne)_{sample} - (^{x}Ne/^{20}Ne)_{atm.}}{(^{x}Ne/^{20}Ne)_{atm.}}$$

Table I-2

Results of Neon Measurements

Fraction	Temperature (°C)	$\frac{^{21}Ne}{^{20}Ne}$ ($\times 10^{-3}$)	δ^{21}* (%)	$\frac{^{22}Ne}{^{20}Ne}$ ($\times 10^{-1}$)	δ^{22}* (%)	^{20}Ne content (# atoms)	^{134}Xe content (# atoms)	Number of fissions
B1	1100	3.04	+ 2.7	1.023	+0.3	5.50×10^{10}	6.92×10^{15}	1.28×10^{17}
B2	1350	2.79	- 5.7	1.056	+3.5	1.58×10^{11}	3.24×10^{15}	
B3	1450	2.84	- 4.0	1.030	+1.0	1.76×10^{11}	1.90×10^{14}	
C1	1100	3.43	+15.9	1.056	+3.5	7.50×10^{10}	6.09×10^{15}	1.34×10^{17}
C2	1350	3.24	+ 9.5	1.021	+0.1	2.44×10^{11}	4.30×10^{15}	
C3	1450	2.96	0.0	1.038	+1.8	2.44×10^{11}	4.20×10^{14}	
Errors:	±50	±6%		±3%		±7%	±7%	
Atmosphere (28):		2.96		1.020				

$$* \delta^{x} = \frac{(^{x}Ne/^{20}Ne)_{sample} - (^{x}Ne/^{20}Ne)_{atm.}}{(^{x}Ne/^{20}Ne)_{atm.}}$$

It is evident that the samples have atmospheric isotope ratios, within experimental errors. The constant positive δ^{22} values lie within the estimated errors and must be ascribed to some small systematic error. The rather large δ^{21} values in sample C can not be considered significant, since any non-atmospheric component would necessarily also be present in sample B.

A correlation plot of cumulative ^{20}Ne vs. cumulative ^{134}Xe content for the different temperature fractions is shown in Fig. I-5. The straight line represents the expected correlation if Ne and Xe were liberated from heated uranium oxide at identical rates. Since Ne is expected to diffuse at least as readily as Xe a more realistic correlation would have to have a larger initial slope. It can be seen that the observed correlation is very different from that expected on the assumption that Ne and Xe have a common origin. Most, if not all, of the observed neon must be of atmospheric origin and probably results from outgassing of the quartz sample vial during extraction. Comparable amounts of neon were found in irradiated blanks.

Upper limits for the formation of neon in fission can be established by considering the precision of the isotope ratio measurements. The criterion used is that a consistent deviation from atmospheric isotope composition

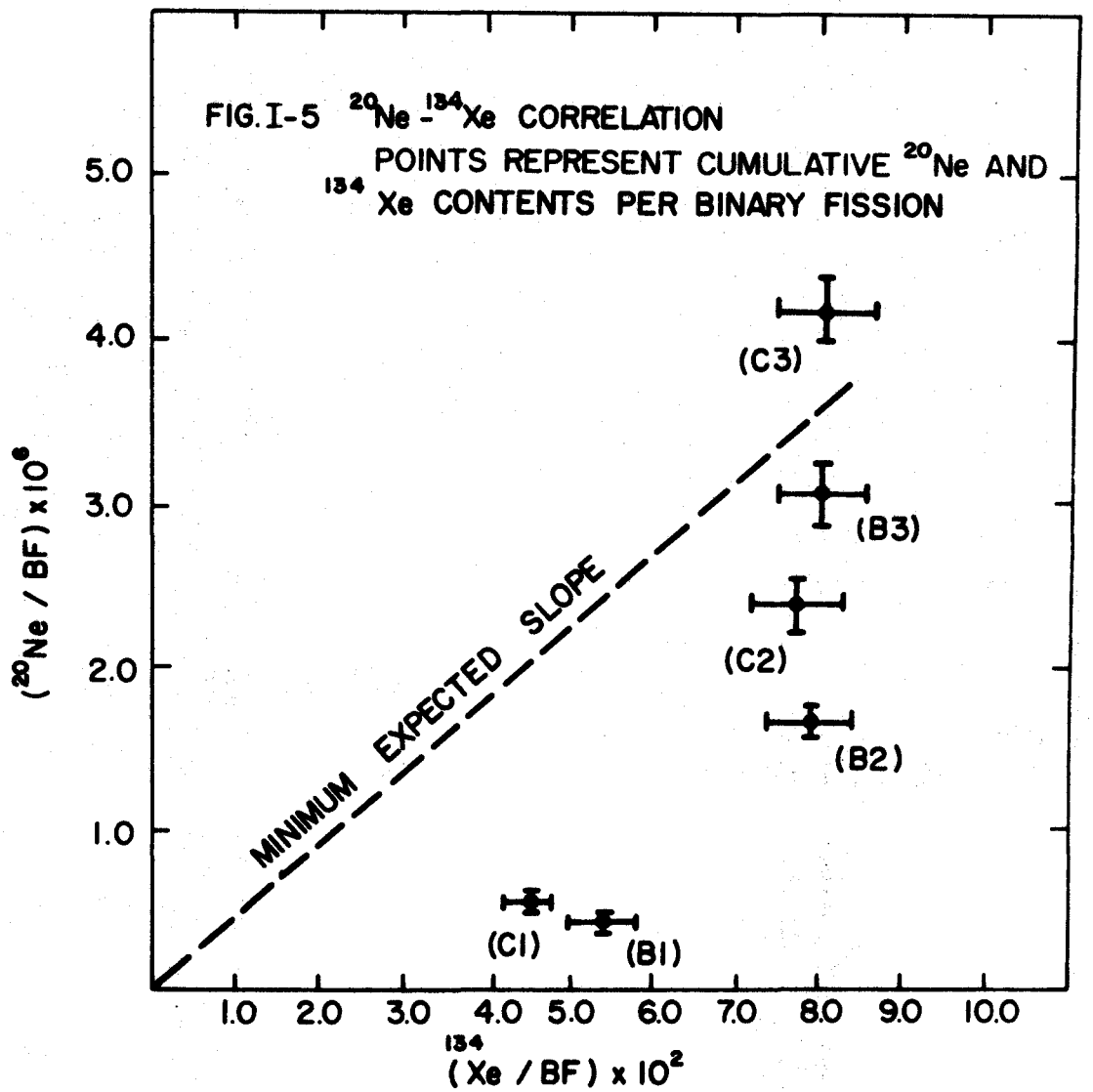
FIG. I-5 ^{20}Ne - ^{134}Xe CORRELATION
POINTS REPRESENT CUMULATIVE ^{20}Ne AND ^{134}Xe CONTENTS PER BINARY FISSION
MINIMUM EXPECTED SLOPE
(C3)
(B3)
(C2)
(B2)
(C1)
(B1)
5.0
4.0
3.0
2.0
1.0
$(^{20}Ne / BF) \times 10^6$
1.0 2.0 3.0 4.0 5.0 6.0 7.0 8.0 9.0 10.0
$(^{134}Xe / BF) \times 10^2$

of three times the estimated error could have easily been detected. (It seems highly improbable that neon isotopes produced in fission would have atmospheric composition.) Therefore an upper limit for the formation of neon in fission is 9% of ^{20}Ne and ^{22}Ne, and 18% of ^{21}Ne actually observed. Only fractions B1 and C1 are considered, since these represent optimum conditions (small atmospheric Ne and large fission Xe components). The upper limits obtained are shown in Table I-3. Since lower limits were obtained for fraction B1, these values were adopted.

B. ARGON MEASUREMENTS

Argon was extracted from all three samples listed in Table I-1. Results of measurements on these are given in Table I-4.

The data reveals at once the presence of some radioactive ^{37}Ar and ^{39}Ar, and a non-atmospheric component of ^{38}Ar. The isotopes ^{36}Ar and ^{40}Ar appear to have close to atmospheric relative abundances. The deviation of the ratios $^{36}Ar/^{40}Ar$ and $^{38}Ar/^{40}Ar$ from atmospheric values are shown in Table I-5. It is seen that the high temperature fractions in each sample show a definite enrichment in ^{38}Ar, whereas ^{36}Ar deviations are both

TABLE I-3

Upper Limits for Neon Yields

Fraction	Isotope	Measured content (# atoms)	Fission* component (# atoms)	^{134}Xe content (# atoms)	$\frac{x_{Ne}}{^{134}Xe}$	$\frac{x_{Ne}}{BF}$**
B1	^{20}Ne	5.50×10^{10}	$<4.95 \times 10^{9}$	6.92×10^{15}	$<7.15 \times 10^{-7}$	$<5.77 \times 10^{-8}$
	^{21}Ne	1.63×10^{8}	$<2.93 \times 10^{7}$		$<4.23 \times 10^{-9}$	$<3.41 \times 10^{-10}$
	^{22}Ne	5.61×10^{9}	$<5.05 \times 10^{8}$		$<7.30 \times 10^{-8}$	$<5.88 \times 10^{-9}$
C1	^{20}Ne	7.50×10^{10}	$<6.75 \times 10^{9}$	6.09×10^{15}	$<1.11 \times 10^{-6}$	$<8.93 \times 10^{-8}$
	^{21}Ne	2.22×10^{8}	$<4.00 \times 10^{7}$		$<6.57 \times 10^{-9}$	$<5.29 \times 10^{-10}$
	^{22}Ne	7.65×10^{9}	$<6.89 \times 10^{8}$		$<1.13 \times 10^{-7}$	$<9.12 \times 10^{-9}$

* 9% and 18% of measured content for ^{20}Ne, ^{22}Ne, and ^{21}Ne, respectively

** BF = Binary Fission

Table I-4

Results of Argon Measurements

Temperature Fraction	(°C)	$\frac{36Ar}{40Ar}$ (x 10^{-3})	$\frac{37Ar}{40Ar}$ (x 10^{-5})	$\frac{38Ar}{40Ar}$ (x 10^{-4})	$\frac{39Ar}{40Ar}$ (x 10^{-5})	$\frac{42Ar}{40Ar}$ (x 10^{-5})	^{40}Ar content (# atoms)	^{134}Xe content (# atoms)	Number of fissions
A1	900	3.45	7.2	6.58	52.3	< 69	1.59×10^{12}	2.38×10^{15}	
A2	1300	3.55	19.2	9.44	641	<3300	6.01×10^{11}	1.84×10^{16}	3.60×10^{17}
A3	1450	3.50	15.2	10.44	750	< 210	5.61×10^{11}	8.25×10^{15}	
B1	1100	3.10	1.0	5.99	2.0	< 2.0	6.52×10^{12}	6.92×10^{15}	
B2	1350	3.33	1.0	7.38	1.6	< 8.0	1.44×10^{12}	3.24×10^{15}	1.28×10^{17}
B3	1450	3.94	0.8	7.55	3.6	< 5.0	8.80×10^{11}	1.90×10^{14}	
C1	1100	3.23	0.8	6.33	1.0	< 9.1	3.10×10^{12}	6.09×10^{15}	
C2	1350	3.15	1.4	6.80	3.0	< 1.1	1.09×10^{12}	4.30×10^{15}	1.34×10^{17}
C3	1450	3.71	0.6	6.93	4.4	< 1.7	3.60×10^{11}	4.20×10^{14}	
Errors:		±3%	±10%	±3%	±10%		±7%	±7%	
Atmosphere (29)		3.38		6.33					

Table I-5

Deviations from atmospheric argon

Fraction	δ^{36}* (‰)	δ^{38}* (‰)	^{40}Ar content (# atoms)
A1	+ 2.1	+ 4.1	1.59×10^{12}
A2	+ 5.0	+49.2	6.01×10^{11}
A3	+ 3.5	+73.0	5.61×10^{11}
B1	- 8.3	- 5.2	6.52×10^{12}
B2	- 1.5	+16.6	1.44×10^{12}
B3	+16.5	+19.3	8.80×10^{11}
C1	- 4.4	0.0	3.10×10^{12}
C2	- 6.8	+ 7.4	1.09×10^{12}
C3	+ 9.8	+ 9.5	3.60×10^{11}

$$* \ \delta^{x} = \frac{(^{x}Ar/^{40}Ar)_{sample} - (^{x}Ar/^{40}Ar)_{atm.}}{(^{x}Ar/^{40}Ar)_{atm.}}$$

positive and negative.

All isotope ratios were normalized to ^{40}Ar and therefore deviations from atmospheric argon are calculated on the assumption that all ^{40}Ar is of atmospheric origin. This assumption is supported by the close agreement between atmospheric $^{36}Ar/^{40}Ar$ and measured $^{36}Ar/^{40}Ar$. Also, the presence of appreciable amounts of fissiogenic ^{40}Ar should be discernible on an ^{40}Ar - ^{134}Xe correlation plot. Such a plot, Fig. I-6, however yields no apparent correlation. On these grounds it is assumed that all of observed ^{40}Ar is of atmospheric origin (it again seems highly improbable that argon isotopes produced in fission would have atmospheric composition).

Absolute amounts of non-atmospheric argon components are shown in Table I-6. Only upper limits are listed for ^{42}Ar. Peaks observed at mass position 42 were due to $^{84}Kr^{++}$. Measurements of the ratio $^{84}Kr^{++}/^{86}Kr^{++}$ yielded the values expected from the known binary fission yields. The limits for ^{42}Ar were set equal to 5% of the observed $^{84}Kr^{++}$ peaks. The large values shown for sample A indicate a poorer separation of Kr from Ar before sample analysis, and hence larger Kr^{++} peaks.

To determine whether the observed non-atmospheric components are due to fission, cumulative contents for the different fractions were calculated and normalized to the

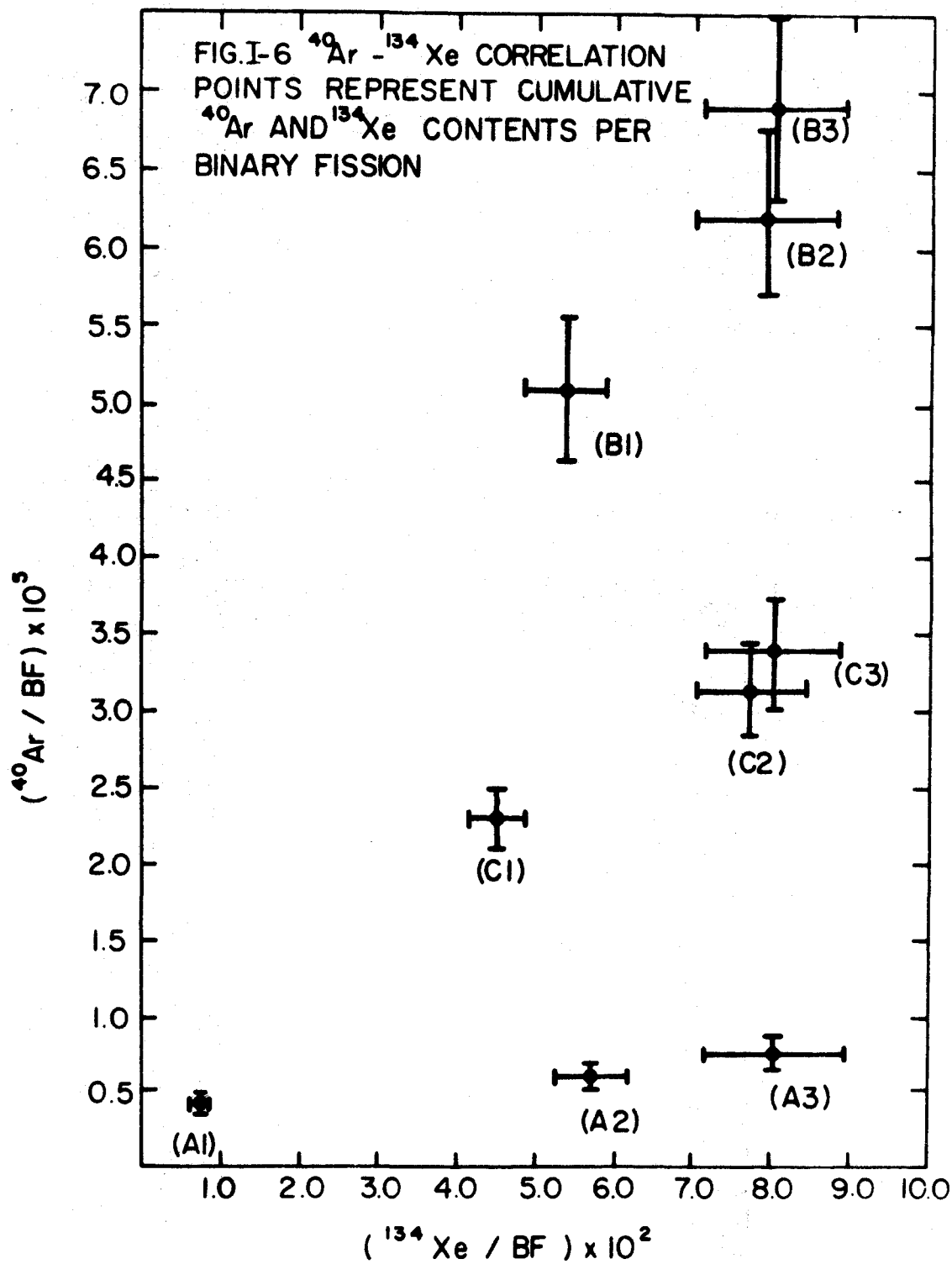
FIG.I-6 ^{40}Ar - ^{134}Xe CORRELATION
POINTS REPRESENT CUMULATIVE
^{40}Ar AND ^{134}Xe CONTENTS PER
BINARY FISSION
(B3)
(B2)
(B1)
(C3)
(C2)
(C1)
(A3)
(A2)
(A1)
7.0
6.5
6.0
5.5
5.0
4.5
4.0
3.5
3.0
2.5
2.0
1.5
1.0
0.5
1.0
2.0
3.0
4.0
5.0
6.0
7.0
8.0
9.0
10.0
$(^{40}Ar / BF) \times 10^{3}$
$(^{134}Xe / BF) \times 10^{2}$

Table I-6

Non-Atmospheric Argon Components

Fraction	^{36}Ar (# atoms) x 10^{8}	^{37}Ar (# atoms) x 10^{7}	^{38}Ar (# atoms) x 10^{7}	^{39}Ar (# atoms) x 10^{7}	^{42}Ar (# atoms) x 10^{7}	^{134}Xe (# atoms) x 10^{15}
A1	1.1	11.4	4.1	83	< 110	2.38
A2	1.0	11.5	18.7	385	<1983	18.40
A3	0.7	8.5	25.9	421	< 118	8.25
Total	2.8	31.4	48.7	889	<2211	29.03
B1	-18.3	6.5	-21.4	13.0	< 13.0	6.92
B2	- 0.7	1.4	15.1	2.3	< 11.5	3.24
B3	4.9	0.7	10.8	3.2	< 4.4	0.19
Total	-14.1	8.6	4.5	18.5	< 28.9	10.35
C1	- 4.6	2.5	0.0	3.1	< 28.2	6.09
C2	- 2.5	1.5	5.1	5.7	< 1.2	4.30
C3	1.2	0.2	2.2	1.6	< 0.6	0.42
Total	- 5.9	4.2	7.3	10.4	< 30.0	10.81

number of fissions in each sample. These values are given in Table I-7. Correlation plots of these non-atmospheric components and ^{134}Xe are shown in Fig. I-7. Again no apparent correlation exists. These argon components must be ascribed to the presence of impurities in the samples and quartz vials during irradiation. Gases extracted from irradiated blanks also contained comparable amounts of these isotopes. In the case of ^{36}Ar the deviations from atmospheric composition must be simply due to measurement errors.

Upper limits for the formation of ^{36}Ar and ^{40}Ar in fission are again based on the criterion that a consistent deviation from atmospheric isotope composition of three times the estimated error (that is a 9% effect) could have been readily detected. The upper limits for other isotopes are set equal to the non-atmospheric components actually observed, or 9% of measured content, whichever is larger. Calculations are based on total Ar and Xe contained in the three fractions of a particular sample. Results are shown in Table I-8.

Table I-9 gives a summary of the upper limits obtained for the production of neon and argon in fission of ^{235}U.

Table I-7

Cumulative Contents and Cumulative Contents/Binary Fission*

	^{36}Ar		^{37}Ar		^{38}Ar		^{39}Ar		^{40}Ar		^{134}Xe	
Fraction	atoms $\times 10^{8}$	$\frac{\text{atoms}}{BF}$ $\times 10^{-10}$	atoms $\times 10^{7}$	$\frac{\text{atoms}}{BF}$ $\times 10^{-10}$	atoms $\times 10^{7}$	$\frac{\text{atoms}}{BF}$ $\times 10^{-10}$	atoms $\times 10^{7}$	$\frac{\text{atoms}}{BF}$ $\times 10^{-10}$	atoms $\times 10^{12}$	$\frac{\text{atoms}}{BF}$ $\times 10^{-5}$	atoms $\times 10^{15}$	$\frac{\text{atoms}}{BF}$ $\times 10^{-2}$
A1	1.1	3.1	11.4	3.17	4.1	1.1	83	23	1.59	0.44	2.4	0.75
A2	2.1	5.8	22.9	6.36	22.8	6.33	468	130	2.19	0.61	20.8	5.77
A3	2.8	7.8	31.4	8.72	48.7	13.53	889	246	2.75	0.76	29.0	8.06
B1	-18.3	-143.	6.5	5.1	-21.4	-16.7	13.0	10.2	6.52	5.09	6.9	5.41
B2	-19.0	-148	7.9	6.2	- 8.3	- 6.5	15.3	12.0	7.96	6.22	10.2	7.94
B3	-14.1	-110	8.6	6.7	+ 4.5	+ 3.5	18.5	14.5	8.84	6.91	10.4	8.06
C1	- 4.6	- 34	2.5	1.9	0.0	0.0	3.1	2.3	3.10	2.31	6.1	4.54
C2	- 7.1	- 53	4.0	3.0	5.1	3.8	8.8	6.6	4.19	3.13	10.4	7.75
C3	- 5.9	- 44	4.2	3.1	7.3	5.5	10.4	7.8	4.55	3.40	10.8	8.06

* For ^{40}Ar total measured amounts are given, whereas for other isotopes only non-atmospheric components are represented.

FIG. I-7. Ar - Xe CORRELATION

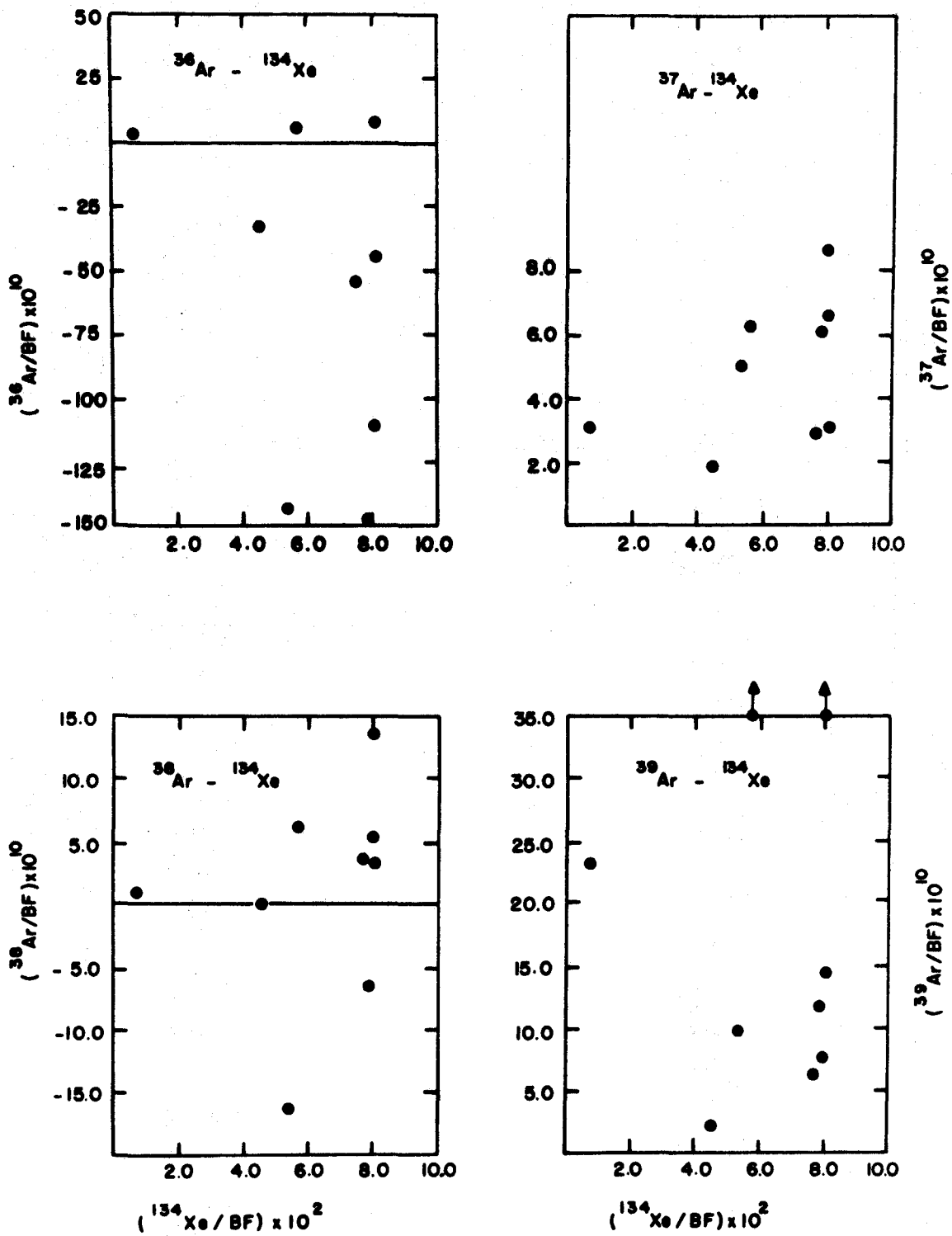

Table I-8

Upper Limits for Argon Yields

Sample	Isotope	Total content (# atoms)	Deviation from atmosphere (%)	Fission* component (# atoms)	Number of fissions in sample	$x_{Ar/BF}$
A	^{36}Ar	9.58×10^{9}	2.9	$<8.62 \times 10^{8}$	3.60×10^{17}	$<2.39 \times 10^{-9}$
	^{37}Ar	3.14×10^{8}	100	$<3.14 \times 10^{8}$		$<8.70 \times 10^{-10}$
	^{38}Ar	2.23×10^{9}	28.2	$<2.23 \times 10^{9}$		$<6.19 \times 10^{-9}$
	^{39}Ar	8.89×10^{9}	100	$<8.89 \times 10^{9}$		$<2.47 \times 10^{-8}$
	^{40}Ar	2.75×10^{12}	0.0	$<2.48 \times 10^{11}$		$<6.88 \times 10^{-7}$
	^{42}Ar	$<2.21 \times 10^{10}$		$<2.21 \times 10^{10}$		$<6.13 \times 10^{-8}$
B	^{36}Ar	2.84×10^{10}	- 4.7	$<2.56 \times 10^{9}$	1.28×10^{17}	$<1.99 \times 10^{-8}$
	^{37}Ar	8.60×10^{7}	100	$<8.60 \times 10^{7}$		$<6.70 \times 10^{-10}$
	^{38}Ar	5.65×10^{9}	1.1	$<5.09 \times 10^{8}$		$<3.97 \times 10^{-9}$
	^{39}Ar	1.85×10^{8}	100	$<1.85 \times 10^{8}$		$<1.44 \times 10^{-9}$
	^{40}Ar	8.84×10^{12}	0.0	$<7.96 \times 10^{11}$		$<6.20 \times 10^{-6}$
	^{42}Ar	$<2.89 \times 10^{8}$		$<2.89 \times 10^{8}$		$<2.25 \times 10^{-9}$

continued

Table I-8 (continued)

Upper Limits for Argon Yields

Sample	Isotope	(# atoms)	Deviation from atmosphere (%)	Fission* component (# atoms)	Number of fissions in sample	$x_{Ar/BF}$
C	^{36}Ar	1.48×10^{10}	- 3.9	$<1.33 \times 10^{9}$	1.34×10^{17}	$<9.91 \times 10^{-9}$
	^{37}Ar	4.20×10^{7}	100	$<4.20 \times 10^{7}$		$<3.14 \times 10^{-10}$
	^{38}Ar	2.95×10^{9}	2.4	$<2.66 \times 10^{8}$		$<1.98 \times 10^{-9}$
	^{39}Ar	1.04×10^{8}	100	$<1.04 \times 10^{8}$		$<7.76 \times 10^{-10}$
	^{40}Ar	4.55×10^{12}	0.0	$<4.10 \times 10^{11}$		$<3.05 \times 10^{-6}$
	^{42}Ar	$<3.00 \times 10^{8}$		$<3.00 \times 10^{8}$		$<2.24 \times 10^{-9}$

* Calculated on the basis of percentage deviation from atmosphere or 9% of total content, whichever is larger.

Table I-9

Summary of upper limits for neon and argon yields

Isotope	$\frac{\#\ atoms}{BF}$	
^{20}Ne	$<5.77 \times 10^{-8}$	(B)**
^{21}Ne	$<3.41 \times 10^{-10}$	(B)
^{22}Ne	$<5.88 \times 10^{-9}$	(B)
^{36}Ar	$<2.39 \times 10^{-9}$	(A)
^{37}Ar*	$<2.20 \times 10^{-9}$	(C)
^{38}Ar	$<1.98 \times 10^{-9}$	(C)
^{39}Ar	$<7.76 \times 10^{-10}$	(C)
^{40}Ar	$<6.88 \times 10^{-7}$	(A)
^{42}Ar	$<2.24 \times 10^{-9}$	(C)

* Corrected for radioactive decay

** Indicates sample from which best limits were obtained

IV

DISCUSSION

Earlier radiochemical studies have failed to establish unambiguous evidence for ternary fission of ^{235}U. All these investigations have only shown upper limits for the formation of certain isotopes in fission, some representing limits for whole mass chains and others for independent nuclide formation. The results of the present work have extended these findings to some mass chains and nuclides not previously investigated. Table I-10 shows results from this study and of others.

The values listed in Table I-10 should be compared with Muga's instrumental results. Muga *et al.* (19) have reported a frequency for ternary fission events of $(7 \pm 2) \times 10^{-6}$ per binary fission of ^{235}U. These workers find that the events are roughly evenly divided between Type I and Type II (Type I/Type II = 0.9 ± 0.1 (18)). Type I events result in the formation of two medium fragments (near mass number 56) and one heavy fragment, whereas Type II result in the formation of one light fragment (in mass region 20 - 40 amu) and two heavy fragments. The nuclides investigated in the present work

Table I-10

Radiochemical and Mass Spectrometric Results for Ternary Fission Yields of ^{235}U

Nuclide	Number of Atoms/Binary Fission			
	This work	Roy (30)	Stoenner and Hillman (21)	Prestwood and Bayhurst (22)**
^{7}Be		$<3 \times 10^{-9}$		$<8.8 \times 10^{-8}$
$^{20}Ne^{*}$	$<5.8 \times 10^{-8}$			
$^{21}Ne^{*}$	$<3.4 \times 10^{-10}$			
$^{22}Ne^{*}$	$<5.9 \times 10^{-9}$			
$^{28}Mg^{*}$		$<4.2 \times 10^{-11}$		$<1 \times 10^{-11}$
^{36}Ar	$<2.4 \times 10^{-9}$			
^{37}Ar	$<2.2 \times 10^{-9}$		$\leq(8 \pm 2) \times 10^{-10}$	
^{38}S				$<8.8 \times 10^{-8}$
$^{38}Ar^{*}$	$<2.0 \times 10^{-9}$			
$^{39}Ar^{*}$	$<7.8 \times 10^{-10}$		$\leq(3.10 \pm 0.02) \times 10^{-9}$	
$^{40}Ar^{*}$	$<6.9 \times 10^{-7}$			
$^{41}Ar^{*}$			$\leq(2.8 \pm 0.2) \times 10^{-11}$	
$^{42}Ar^{*}$	$<2.2 \times 10^{-9}$		$\leq(1.1 \pm 1.7) \times 10^{-13}$	

... continued

Table I-10 (continued)

Radiochemical and Mass Spectrometric Results for Ternary Fission Yields of ^{235}U

Nuclide	Number of Atoms/Binary Fission			
	This work	Roy (30)	Stoenner and Hillman (21)	Prestwood and Bayhurst (22)**
^{48}Sc			$\leq(4 \pm 4) \times 10^{-10}$	$<8.8 \times 10^{-8}$
^{51}Cr				
^{54}Mn				
^{56}Mn*				
^{56}Co				
^{57}Co				
^{58}Co				
^{59}Fe*				
^{60}Co				
^{66}Ni*		$=(2.0 \pm 1.0) \times 10^{-10}$		

* Represents chain yield

** Reference (22) states that limits range from 10^{-11} atoms/binary fission for ^{28}Mg to 8.8×10^{-8} for ^{60}Co, but does not give limits for other isotopes separately. The highest limit is shown for all nuclides except ^{28}Mg.

are expected to be Type II products, the total yield of which is measured by Muga et al. to be 3.7×10^{-6} atoms/binary fission. The mass distribution for Type II events taken from (19) and corresponding radiochemical and mass spectrometric limits are shown in Fig. I-8.

Except for ^{20}Ne and ^{40}Ar the limits set by the present work and radiochemical studies are from one to six orders of magnitude lower than Muga's mass distribution would suggest. This apparent inconsistency could be resolved, as suggested by Muga et al., if the true mass distribution were very narrow, perhaps involving unique mass formation, such that detection of this product has as yet escaped the radiochemical and mass-spectrometric investigations. Indeed Muga et al. account for the width of their mass distribution to a large extent by the finite angles subtended by the detectors used in their triple coincidence studies. Also, these experimenters suggest that the ternary fission products may be formed very close to the line of stability, or in fact be formed stable, and may therefore have escaped detection by radiochemical means. Their reasoning derives from considerations of the energies involved. From semi-empirical mass equations one expects about 20 Mev more energy liberated in ternary fission than in binary fission. The total kinetic energies of the three fragments measured by

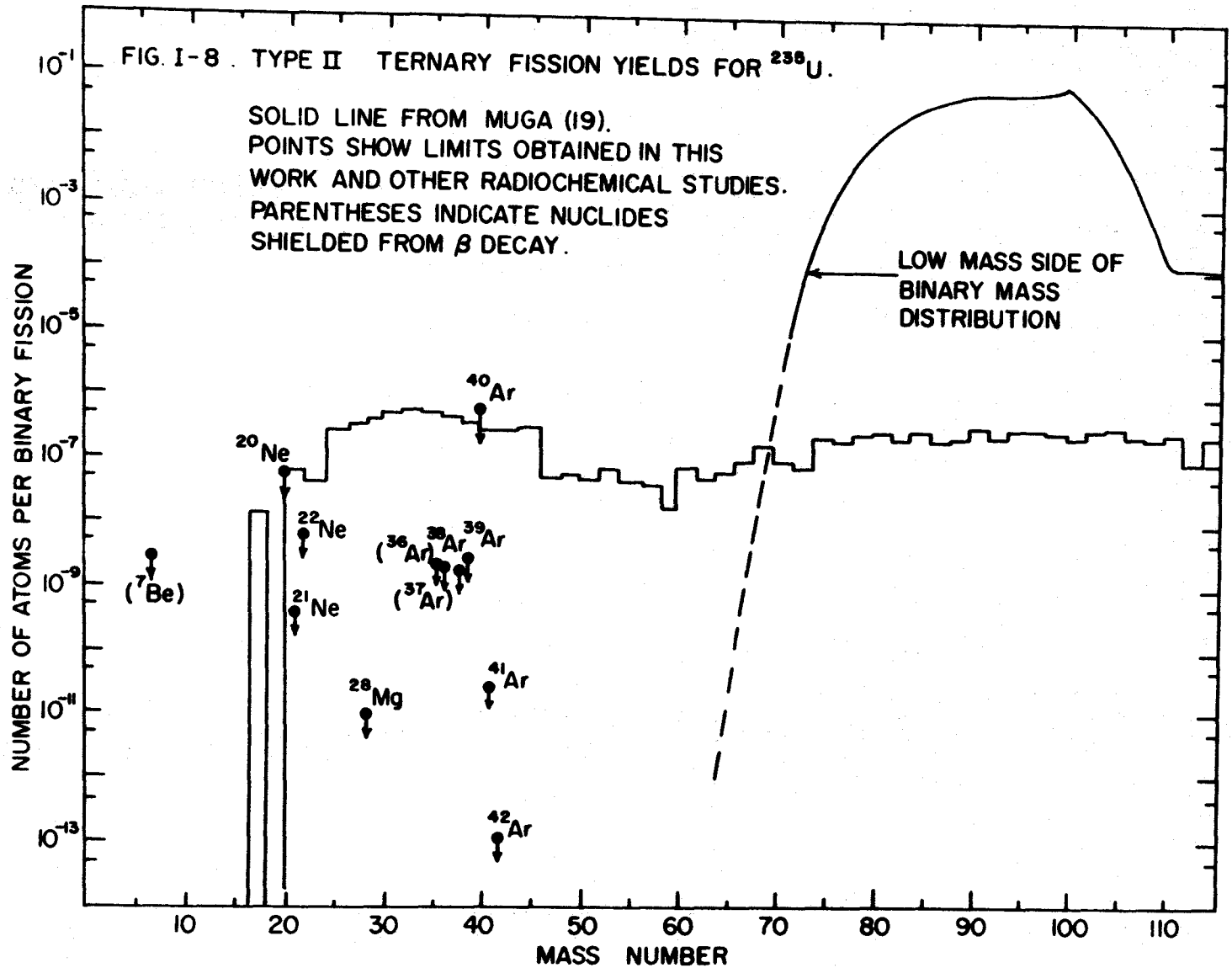
FIG. I-8 . TYPE II TERNARY FISSION YIELDS FOR ^{238}U.
SOLID LINE FROM MUGA (19).
POINTS SHOW LIMITS OBTAINED IN THIS WORK AND OTHER RADIOCHEMICAL STUDIES.
PARENTHESES INDICATE NUCLIDES SHIELDED FROM β DECAY.
LOW MASS SIDE OF BINARY MASS DISTRIBUTION
NUMBER OF ATOMS PER BINARY FISSION
MASS NUMBER
10^{-1}
10^{-3}
10^{-5}
10^{-7}
10^{-9}
10^{-11}
10^{-13}
10
20
30
40
50
60
70
80
90
100
110
^{40}Ar
^{20}Ne
^{22}Ne
(^{36}Ar)
^{38}Ar
^{39}Ar
(^{7}Be)
^{21}Ne
(^{37}Ar)
^{28}Mg
^{41}Ar
^{42}Ar

Muga et al. are however about 10 Mev lower than in the case of binary fission. Therefore Muga et al. argue that ternary fission products, or at least one of these, may be so highly excited (about 50 Mev of excitation energy is available) that rapid neutron evaporation could result in a stable product.

The present study enabled the search for some possible stable end products, but the generally low limits obtained make only ^{20}Ne and ^{40}Ar possible candidates for ternary fission products. The peak of Muga's mass distribution lies closer to mass 40 than 20, and since a broad distribution is ruled out by the low limits of intermediary nuclides attention is focussed on mass 40.

The limits for ^{39}Ar and ^{41}Ar are about two and four orders of magnitude, respectively, lower than for ^{40}Ar. Therefore one would expect unique mass formation at mass position 40. If such were the case, however, the yield of ^{40}Ar should be equal to the total yield of Type II events measured by Muga et al., that is 3.7×10^{-6} atoms/binary fission. The upper limit obtained for ^{40}Ar in this study ($<6.9 \times 10^{-7}$) is lower than this value by more than a factor of five. Unique formation of ^{40}Ar in ternary fission of ^{235}U in amounts implied by the results of Muga et al. appears ruled out by the present study.

A recent evaluation of the experiments carried out by Muga et al. has been made by Steinberg et al. (31). The latter group has shown that scattering events in Muga's triple coincidence studies have not been effectively eliminated and may contribute significantly to the results. In view of such alternative evaluations of the instrumental data the negative results obtained in this work and in earlier radiochemical studies suggest that ternary fission at low excitation energies is either absent or occurs much less frequently than indicated by the instrumental results. Since, however, mass-spectrometric and radiochemical investigations have eliminated only twelve out of a possible forty mass chains the problem of the existence of ternary fission at low excitation energies is still not resolved.

The upper limits obtained for the neon isotopes should also be compared with the findings of Natowitz et al. (32). Using mica and Lexan track detectors this group studied long range fragments from the decay of ^{252}Cf. B, C, N, and O nuclei were observed as products in spontaneous fission with integrated yields $\gtrsim 18 \times 10^{-6}$ atoms/BF. Species with $8 < Z < 13$ were observed with integrated yield $\gtrsim 3 \times 10^{-6}$ atoms/BF. ^{20}Ne, ^{21}Ne, ^{22}Ne and respective precursors ^{20}F, ^{21}F, ^{22}F are expected to be among these products. Assuming a distribution of equal yields over about 10 nuclides in this region one would expect yields

$>3 \times 10^{-7}$ atoms/BF for the three stable neon isotopes. The limits obtained in this work for ^{235}U are from one to three orders of magnitude lower. Although the high yields for ^{252}Cf need confirmation, there is a suggestion of a large systematic difference between ^{235}U and ^{252}Cf fission.

The low limits for ^{38}Ar production in fission of ^{235}U may also be relevant to the studies of ^{38}Ar anomalies in uranium bearing minerals mentioned in the introduction (23, 24, 25). All workers have noted the existence of excess ^{38}Ar in uranium minerals, but whereas Fleming and Thode (23), and Wetherill (24) consider the reactions $^{35}Cl\ (\alpha,p)\ ^{38}Ar$ and $^{35}Cl\ (\alpha,n)\ ^{38}K \xrightarrow{\beta^+} {}^{38}Ar$ to be the most likely sources of excess ^{38}Ar, Shukolyukov et al. (25) attribute this excess directly to spontaneous fission of ^{238}U. The formation of ^{38}Ar by spontaneous fission is not unequivocally ruled out by the present findings for neutron induced fission of ^{235}U. If these suggested differences in fission systematics between ^{235}U and ^{238}U are confirmed by future work they may indicate a greater influence of underlying shell structure during selection of fragments in spontaneously fissioning systems (^{38}Ar has magic neutron number). On the other hand the negative results from this work should prompt renewed investigations into production of argon isotopes in uranium minerals.

PART II

^{3}H, ^{3}He, AND ^{4}He PRODUCED IN FISSION OF ^{235}U

I

INTRODUCTION

A. LONG-RANGE PARTICLE EMISSION

Emission of long-range light charged particles ($Z < 10$) in coincidence with two heavy fission fragments occurs roughly once in several hundred fissions. This type of ternary fission was first observed by Alvarez (7) in 1943 and his discovery was followed by numerous investigations using nuclear emulsions and coincidence techniques (33). The early studies showed that most of the light particles emitted had range and ionization characteristics which were clearly those of alpha particles. Track studies also revealed that these particles originate in the central region of the heavy fragment tracks and are emitted at nearly right angles to these tracks. An analysis of these observations led Tsien (34) to suggest that these particles must be released in the space between the primary fragments at the instant of fission. The energy and angular distributions are then largely determined by the Coulomb field of the two heavy fragments.

Particles other than helium nuclei have also been observed as ternary fission products. Hill (35) first reported protons and Albenesius (36) observed tritons formed in fission of ^{235}U. More recently, counter telescopes with dE/dx detectors as particle identifiers have been employed and a number of other particles have been detected. ^{1}H, ^{2}H, ^{3}H, ^{4}He, ^{6}He, ^{8}He, and Li, Be, B, C, N, and O ions have been observed in both ^{235}U and ^{252}Cf fission. (Feather (37) has reviewed recent studies in ternary fission).

Energy and angular distributions have been measured for some of these particles. Gazit et al. (38) have obtained partial energy spectra for all observed particles with $Z > 2$ in the case of ^{252}Cf. Due to necessary shielding of the detectors from natural alpha particles, fission fragments, and other background effects, studies of energy distributions usually have a rather large low-energy cut-off and hence omit the low energy portion altogether. All energy spectra appear to have gaussian shape (centred at ~16 and 8 Mev for ^{4}He and ^{3}H, respectively), and where angular distributions have been measured these show a peaking at about 82° with respect to the direction of the lighter of the two heavy fragments. For alpha particles variations of most probable energy with angle of emission have also been measured (39, 40). Using such data

trajectory calculations have been carried out (39, 41, 42) in an attempt to establish initial dynamical parameters which yield the observed distributions. The picture which has emerged from these studies is that the light particle is emitted isotropically either at the instant of scission, or very shortly thereafter ($<10^{-21}$ sec), in the region between the two heavy fragments, and has an initial kinetic energy of 2 to 3 Mev. At the instant the particle materializes the centres of the two heavy fragments are from 20 to 25 x 10^{-15} m apart. A common mechanism appears operative for all light particles although different initial conditions are required for the various cases.

Experimental studies of absolute and relative yields of the light particles will ultimately provide a crucial test for any dynamical theory of fission. With this view yields of the long-range particles have been measured at various excitation energies and for several different fissioning nuclides. Results obtained to date, however, lack good statistical accuracy and fluctuate widely for individual cases. For slow neutron fission of ^{235}U reported yields for alpha particles emitted per fission range from one in 230 (43) to one in 505 $\pm$ 50 (44). Nobles (45) has shown, however, that an inverse correlation between long-range particle yield and excitation energy in a given nuclide as well as a trend of increasing

probability of emission with increasing Z^2/A exists.

Reported relative yields for some of the particles also vary by a factor of two or more. A correlation between the probability of formation and the release energy required for a particular particle is expected. An explanation based on evaporation theory is considered inadequate by Halpern (46). Estimates of the release energies for some particles have been made by Halpern (46) and by Feather (47) but differ somewhat in approach and values obtained. Whetstone and Thomas (48) have also estimated release energies based on Halpern's model and have shown a rough dependence of measured yields according to $\exp(-E_r/T)$, where E_r is the release energy, and T corresponds to a nuclear temperature.

The yield of ^3He is considered of some interest. Estimates of release energies for ^3He, ^4He, and Li and Be isotopes given by Whetstone and Thomas predict a ratio of $^3He/^4He$ of $\sim 4 \times 10^{-4}$ (assuming the $\exp(-E_r/T)$ dependence). A precise determination of the $^3He/^4He$ ratio would therefore serve as a test of the yield - release energy correlation over several orders of magnitude. Also, ^3He is estimated to be energetically favoured over any Li or Be isotopes and is therefore expected to have higher yield. For ^{252}Cf Cosper et al. (49) have shown, however, that Li and Be ions are emitted in greater abundance than ^3He (measured

$^{3}He/^{4}He \leq 7.5 \times 10^{-4}$). On the other hand, Cambiaghi et al. (50) have found a much higher yield for ^{3}He ($^{3}He/^{4}He = 1.8 \times 10^{-2}$) than for total Li and Be ions produced in fission of ^{233}U.

The only radiochemical study made of light ternary fission products was that by Albenesius (36) on ^{3}H in ^{235}U fission. Other methods do not achieve completely unambiguous particle identification. The results for ^{3}He mentioned above were obtained using systems of dE/dx and E detectors and it is possible that complete discrimination of ^{3}He from the much more abundant ^{4}He particles was not achieved. Mass spectrometry can give positive identification of different isotopes with widely differing abundances. This technique was used in the present work to measure absolute and relative yields of ^{3}H, ^{3}He, and ^{4}He produced in thermal neutron fission of ^{235}U.

B. SHORT-RANGE PARTICLE EMISSION

Emission of short-range light charged particles in fission of ^{235}U was first observed by Cassels et al. (51) using proportional counters in coincidence. The particles were tentatively identified as alpha particles having an energy of ~1 Mev. Assuming isotropic emission

a probability of occurrence of one in 30 fissions was assigned. Noting the emission to be predominantly at right angles to the heavy fragment tracks Green and Livesey (52) later corrected this value to one in 90 fissions. These workers, using nuclear emulsions, measured a frequency of one in 100 $\pm$ 30 fission events.

Studies of these low energy particles have been carried out only with nuclear emulsions and proportional counters in coincidence. Low mass nuclear recoils and scattered fission fragments can sometimes not be distinguished from true events in such experiments. The preponderance of short tracks at ~90° to the heavy fragment tracks was, however, considered evidence by Tsien et al. (53) that some of the short tracks are due to light particles emitted in fission. A frequency of emission of 1.1×10^{-2} per binary fission was established by these workers. Titterton (54) and Allen and Dewan (55) observed these short-range particles in ^{235}U fission with frequencies of one in 85 $\pm$ 10 and one in 76 $\pm$ 8 fissions, respectively. Both groups suggested that some of the particles were heavier than alpha particles. Muga et al. (56) also observed such events in ^{252}Cf fission but did not determine their frequency of occurrence. The study of these particles has been entirely omitted in the numerous recent experiments on long-range particles and no mechanism for the release of

these particles has been suggested to date.

The present experiments to measure yields of ^{3}H, ^{3}He, and ^{4}He from ^{235}U fission were designed to enable separate detection of long-range and possible short-range components of these particles.

II

EXPERIMENTAL

A. PREPARATION OF SAMPLES

(i) Thick catcher foil experiment.

Samples of ^{235}U weighing a few tenths of a mg were prepared by evaporation of weak uranyl nitrate solution onto Pb foil. The thickness of the fission source was ~1 mg/cm^2 and permitted recoil of all fission fragments into the Pb catcher foils. Individual Pb foils were ~30 mg/cm^2 thick and placed together to give a total thickness of ~330 mg/cm^2, sufficient to stop alpha particles and tritons of 40 and 14 Mev, respectively. The thick sample foil assembly was folded, sealed in a quartz ampoule, along with blank Pb foil, and irradiated for about ten days at a flux of ~1.5 x 10^{13} neutrons/cm^2/sec. Some samples were wrapped with Cd to permit determination of possible contributions to ^3H and He due to fast neutrons. Further test samples consisted of depleted ^{238}U prepared in identical manner to the ^{235}U samples.

Pb foils were chosen because of the relatively low (n, α) and (n, t) cross sections of Pb. Another factor

in the choice of Pb was its relatively low melting and boiling points, which enabled easy extraction of He from the foils.

Details of all samples are given in Table II-1. Series A was used to measure $^{3}He/^{4}He$ as a function of cooling time, as well as total ^{4}He content. Series B served as a check on possible diffusion effects caused by heating the Pb foils during irradiation. Series C was wrapped with Cd, and series D consisted of depleted ^{238}U. Series E was part of the stacked foil experiment to be described below.

(ii) Stacked foil experiment.

In order to separate possible short-range components of the light particles stacks of Pb foils were arranged in such a way that He contents could be measured for each foil individually. The method is similar to that used by Douthett and Templeton (76) to measure ranges of fragments from high-energy fission of uranium. The geometrical arrangement is shown in Fig. II-1. This method, as adapted for the present work, enables measurement of the integral range distributions of the He isotopes. Knowledge of range-energy relations can then be used to yield energy distributions. All short-range particles will be stopped

Table II-1

Sample Details

Sample	Weight	Irradiation Period (days)	Cooling Period (days)
A1	0.2 mg ^{235}U	10	3.5
A2	0.2	10	7.5
A3	0.2	10	12
A4	0.2	10	17.5
A5	0.2	10	25
A6	0.2	10	35
A7	0.2	10	39
B1	0.1	10	35
B2	0.3	10	35
B3	0.4	10	35
B4	0.5	10	35
C1*	0.2	8	6
C2*	0.2	8	6
D1	0.2 mg ^{238}U	8	10
D2	0.2 mg ^{238}U	8	10
E1	0.4 mg ^{235}U	22	5
E2	0.4	22	37
E3	0.6	22	48

* Cd wrapped (~1 mm thick)

FIG. II-1. FOIL STACK ASSEMBLY.

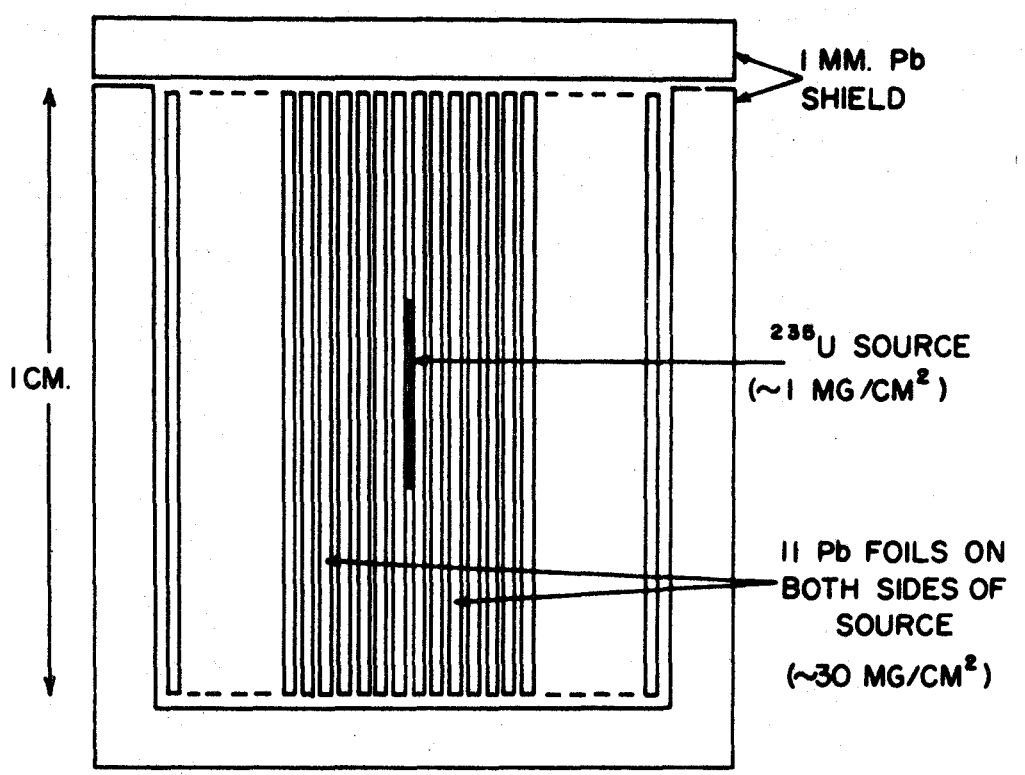

in the first foil, which should therefore exhibit an anomolously high content of these particles. The method has the advantage that it requires no collimator and hence greatly improved sensitivity is attained.

In Appendix A it is shown that the number of particles found in the i^{th} foil will be

$$N_i = a_1 + a_2 \left[\Delta t_i \int_{E(t_i)}^{\infty} \frac{n(E)\ dE}{r(E)} + \right.$$

$$\left. + \int_{E(t_{i-1})}^{E(t_i)} \frac{(r(E) - t_{i-1})}{r(E)}\ n(E)\ dE \right] \qquad (1)$$

where, N_i = number of particles in i^{th} foil

a_1 = constant background found in each foil

a_2 = constant depending on source strength

Δt_i = thickness of i^{th} foil

t_i = total foil thickness up to and including the i^{th} foil

$E(t_i)$ = energy of particle with range t_i

$n(E)$ = energy distribution of particles

$r(E)$ = range of particle with energy E

The parameters for n(E) are determined when data points N_i are fit with equation (1).

N_i was obtained from mass spectrometric measurement of the amounts of ^3He and ^4He present in each foil. t_i and Δt_i were determined by weighing foils of known area.

(iii) Extraction of He from Pb foils.

He as well as Kr and Xe were extracted from the Pb foils by vaporizing in vacuum. The extraction system used was essentially that described in Part I of this thesis for the extraction of Ne and Ar from uranium oxide.

The Pb foils were dropped into a Mullite tube sealed to the sample inlet system of the mass spectrometer. The tube was held at 750° C with a resistance furnace. He released upon vaporization of the foils was allowed to expand into evacuated flasks. Kr and Xe were condensed on activated charcoal held at liquid nitrogen temperature. The sample flasks containing evolved He were sealed onto the inlet system of the mass spectrometer and analyzed within one hour of extraction. Early analysis was necessary because He diffuses appreciably through Pyrex glass. Blank runs however showed that within two hours of sealing an evacuated pyrex flask (200 ml volume, 1 mm wall thickness) no detectable amounts of atmospheric He had diffused into the flasks.

B. MASS SPECTROMETRY

Procedures employed in this phase of the experiment were essentially the same as those described in Part I for Ne and Ar analyses. Only features peculiar to He analyses will be mentioned here.

The presence of HD and H_3 are undesirable backgrounds. When analyzing small samples of ^3He this isobaric contamination must be held to a minimum. A Ti getter incorporated into the mass spectrometer vacuum system, and kept at room temperature during analyses, greatly lowered the HD-H_3 background. The HD-H_3 peak was usually about five times the sample ^3He, at which levels ^3He was totally resolved.

Calibration of the mass spectrometer for peak height response and mass discrimination was achieved by analyzing atmospheric He prepared from aliquots of air of known volume immediately after each fission He sample. A concentration for He in the atmosphere of 5.24 ppm (57) and a ratio of $^3He/^4He = 1.37 \times 10^{-6}$ (58) were assumed.

The number of fissions in each sample was determined by measurement of the ^{86}Kr content.

III

RESULTS

A. MEASUREMENT OF $^3He/^4He$ AND ABSOLUTE He CONTENT

(i) $^3He/^4He$ as a function of cooling period.

It was originally anticipated that measurement of $^3He/^4He$ as a function of cooling period should yield the contributions to ^3He due to both independent formation of ^3He in fission as well as decay of ^3H produced in fission. Samples of series A (see Table II-1) were prepared and analyzed for this purpose.

Irradiation of all series A samples was simultaneous, but extraction and analysis of He was carried out at different times. Fig. II-2 shows typical traces of mass spectra obtained for samples A2 and A7, which represent cooling periods of 7.5 and 39 days, respectively. Results of all samples of series A are listed in Table II-2 and plotted as a function of T (cooling period) in Fig. II-3.

Due to the relatively long half-life of ^3H (12.26 years) the ratio $^3He/^4He$ is expected to increase

FIG. II-2. HELIUM MASS SPECTRA AT DIFFERENT COOLING PERIODS.

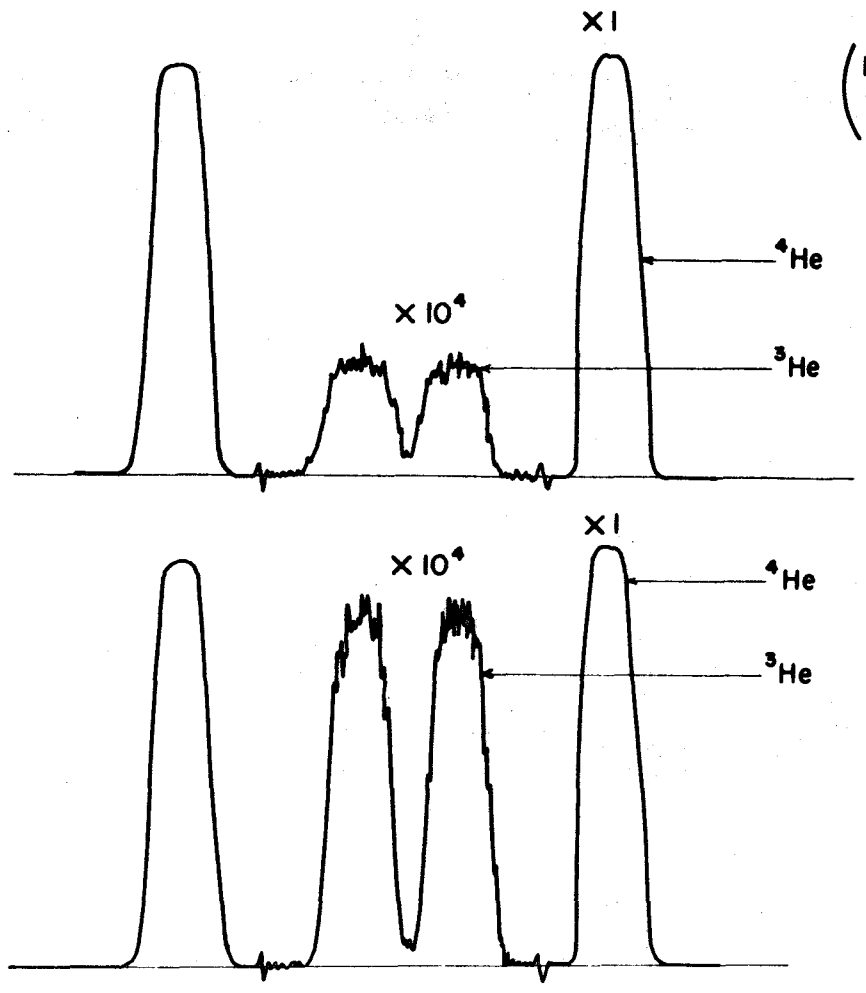

Table II-2

Results of $^{3}He/^{4}He$ measurements

Sample*	Cooling Period (hours)	$^{3}He/^{4}He$ ($\times 10^{-5}$)
A1	85	2.08 ± 0.31
A2	180	3.23 ± 0.48
A3	285	4.90 ± 0.49
A4	422	5.53 ± 0.55
A5	593	7.55 ± 0.60
A6	836	11.17 ± 0.89
A7	949	10.06 ± 0.80

*All samples contained 0.2 mg ^{235}U and were irradiated simultaneously for 10 days.

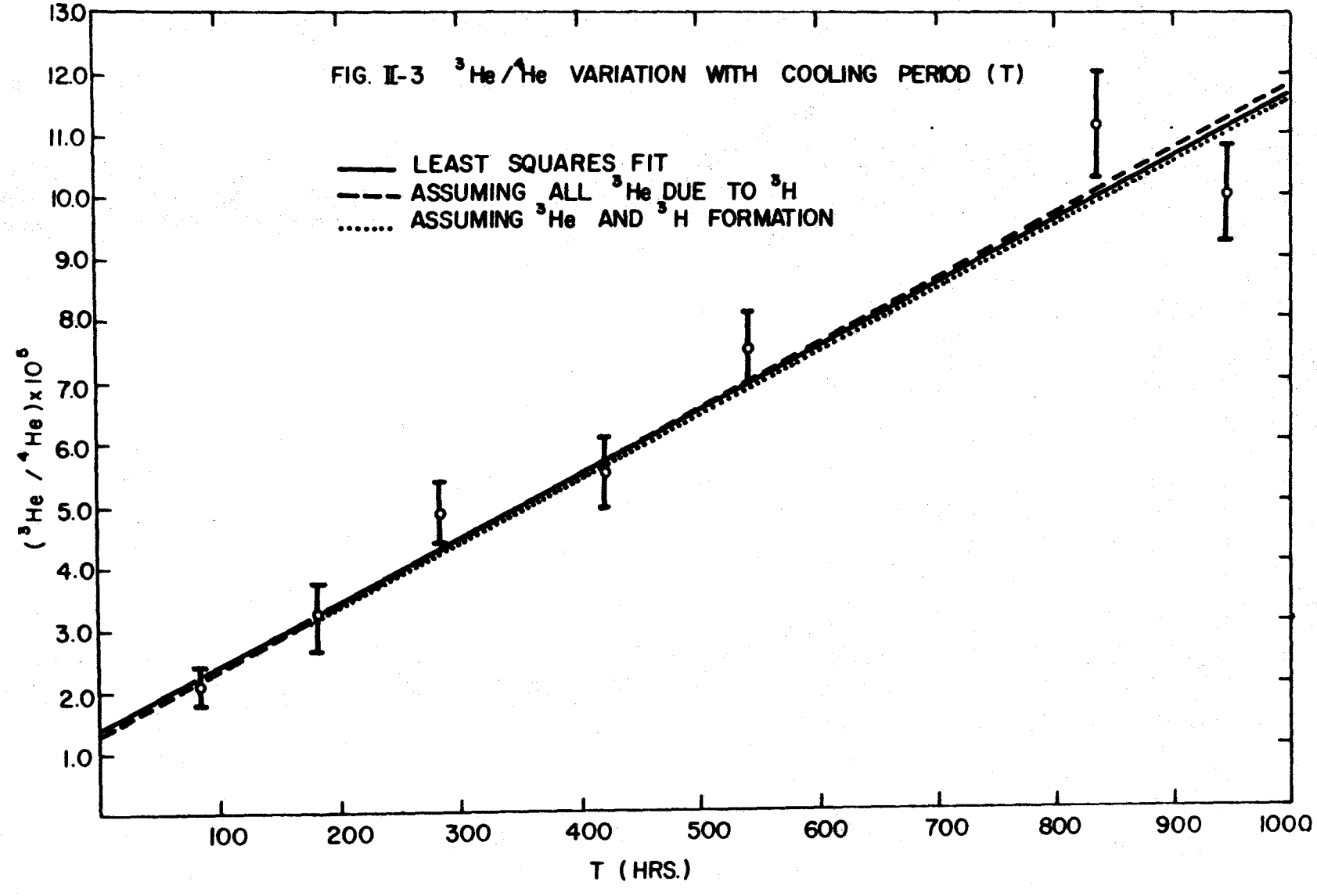
FIG. II-3 $^3He/^4He$ VARIATION WITH COOLING PERIOD (T)
LEAST SQUARES FIT
ASSUMING ALL ^3He DUE TO ^3H
ASSUMING ^3He AND ^3H FORMATION
$(^3He/^4He) \times 10^5$
T (HRS.)
13.0
12.0
11.0
10.0
9.0
8.0
7.0
6.0
5.0
4.0
3.0
2.0
1.0
100
200
300
400
500
600
700
800
900
1000

linearly over short cooling periods. In Fig. II-3 the least squares fit to the data points yields a straight line with intercept and slope of $(1.38 \pm 0.29) \times 10^{-5}$ and $(0.0103 \pm 0.0007) \times 10^{-5}$/hr respectively. The slope of the straight line is determined by the $^{3}H/^{4}He$ ratio as well as $T_{1/2}$ for ^{3}H. The intercept, on the other hand, depends on $^{3}H/^{4}He$, $T_{1/2}$ of ^{3}H, and a possible component of $^{3}He/^{4}He$ due to independent formation of ^{3}He. Using the experimentally obtained slope, and $T_{1/2}(^{3}H) =$ 12.262 y (59), one calculates $^{3}H/^{4}He = 1.60 \times 10^{-2}$, which in turn should yield an intercept at T = 0 of 1.27×10^{-5}. The difference between this value and the experimental intercept may be taken as the component of $^{3}He/^{4}He$ due to direct formation of ^{3}He, that is $^{3}He/^{4}He = (1 \pm {}^{3}_{1}) \times 10^{-6}$.

Alternatively, the ^{3}He may be entirely due to ^{3}H decay. The dashed line in Fig. II-3 was obtained by correcting each data point for growth of ^{3}He from ^{3}H, calculating the T = 0 intercept from the weighted mean, and using the known half-life of ^{3}H to determine the slope of the straight line. It is seen that this line very nearly coincides with the least squares fit to the experimental points.

Assuming two components for ^{3}He production in fission, however, the relative yields (to be corrected for

short-range component later) are measured to be:

$$^{3}H/^{4}He = (1.60 \pm 0.37) \times 10^{-2}$$
$$^{3}He/^{4}He = (1 \,^{+\,3}_{-\,1}) \times 10^{-6}$$

(ii) Frequency of formation of ^{4}He.

The ratio $^{4}He/BF$ (BF = binary fission) was determined from absolute measurements of ^{4}He and ^{86}Kr contents. A fission yield of 2.04 % was assumed for ^{86}Kr (27). Values obtained from all samples of series A and B, as well as one value from series E, are listed in Table II-3.

The mean value of $(4.27 \pm 0.12) \times 10^{-3}$ obtained for $^{4}He/BF$ in Table II-3 corresponds to a frequency of formation of one ^{4}He atom in 234 ± 7 fissions. This represents total ^{4}He produced. Relative contributions from short-range and long-range ^{4}He components will be discussed in part B of this chapter.

(iii) Check on possible diffusion effects.

Diffusion of ^{3}H or He out of the Pb catcher foils during irradiation could result from local heating caused

Table II-3

Frequency of formation of ^4He

Sample	$^4He/BF$ ($\times 10^{-3}$)
A1	3.86*
A2	3.84
A3	3.95
A4	3.60
A5	4.97
A6	4.73
A7	4.62
B1	4.20
B2	4.24
B3	4.70
B4	4.36
E**	4.17
mean	4.27 ± 0.12***

* Estimated total error of individual measurements is 8%

** Obtained by combining data from E1 and E2

***Indicated error is standard deviation of the mean

by the fission source. It was considered necessary to investigate this effect.

Diffusion phenomena show strong temperature dependence. Fission sources of different strengths, prepared on identical catcher foils, should therefore exhibit varying diffusion losses, if they occur at measurable levels. Series B samples, plus sample A6 (see Table II-1), consisted of ^{235}U sources varying in weight by as much as a factor of five. Irradiation of these sources was simultaneous and extraction and analysis of He was carried out on the same day. Results of $^{3}He/^{4}He$ measurements on these samples are given in Table II-4. It is seen that the ratios have a constant value, within experimental errors. Therefore it may be assumed that no diffusion losses occurred.

Later measurement of the $^{4}He/^{86}Kr$ ratios also yielded constant values, within errors, and served as additional evidence against appreciable diffusion losses.

(iv) Contributions to observed He from reactions other than fission.

The possibility that some of the He extracted from the catcher foils is due to (n, α) or (n, t) reactions

Table II-4

Results of $^{3}He/^{4}He$ measurements for different source strengths

Sample*	Weight of ^{235}U (mg)	$^{3}He/^{4}He$** ($\times 10^{-4}$)
B1	0.1	1.10 ± 0.07
A6	0.2	1.12 ± 0.07
B2	0.3	1.05 ± 0.06
B3	0.4	1.08 ± 0.07
B4	0.5	1.19 ± 0.07
mean		1.11 ± 0.05

* All samples were irradiated simultaneously for 10 days, and permitted to cool for 35 days.

** Errors for individual values are estimated measurement errors of ± 6%.

involving targets in the Pb foils, or the source itself, had to be considered. For this investigation blank Pb foils of identical weights to the sample foils were irradiated along with each sample. In addition, two foils loaded with 0.2 mg ^{235}U and wrapped with Cd (series C), as well as two samples consisting of 0.2 mg of depleted ^{238}U (series D) were irradiated.

All blank foils contained some ^{3}He and ^{4}He. These amounts ranged from ~5 to 15% of total observed values, for both isotopes. Appropriate corrections were applied to all measured samples. Small fluctuations of He contents in the blanks were included in the estimated errors for the $^{3}He/^{4}He$ and total He measurements.

The two Cd wrapped samples contained ~4 and 6% of the ^{4}He found in identical samples exposed to the total neutron spectrum. Such amounts may be ascribed to fast neutron fission. ^{3}He extracted from these samples was barely measurable above the ^{3}He attributed to blank foils, but appeared to have roughly the same porportion to ^{4}He as measured in other samples.

The samples of depleted ^{238}U contained no measurable amounts of ^{3}He or ^{4}He after irradiation.

These experiments strongly indicate a direct correlation between the observed He isotopes and thermal neutron fission of ^{235}U.

B. RESULTS OF STACKED FOIL EXPERIMENT

Two stacked foil assemblies were prepared for the purpose of energy distribution measurements on ^{3}H and ^{4}He. Samples E1 and E2 (see Table II-1 and Fig. II-1) were series of foils taken from opposite sides of the same ^{235}U fission source. Sample E3 is a series of foils taken from one side of a second fission source. The series of foils opposite E3, as well as foil #1 of E3, was accidentally damaged and could not be used in any measurements. Useful results covering the whole energy spectrum for ^{4}He were obtained from E1 and E2, and for ^{3}H from E2 only. Since the first foil from E3 was lost, and unusually high HD-H_3 background caused problems with the ^{3}He measurements, only the long-range ^{4}He component was determined from this series.

The ^{4}He and ^{3}H contents for sample E2 are plotted as a function of foil number in Figs. II-4 and II-5, respectively (the relative amounts of ^{3}H in each foil were obtained from the relative amounts of ^{3}He in each foil, the ^{3}He being due to in situ decay of ^{3}H). Ranges and energies corresponding to foil numbers are also shown. Range-energy data for ^{4}He and ^{3}H were taken from Whaling (60) and Williamson, Boujot, and Picard (61), respectively.

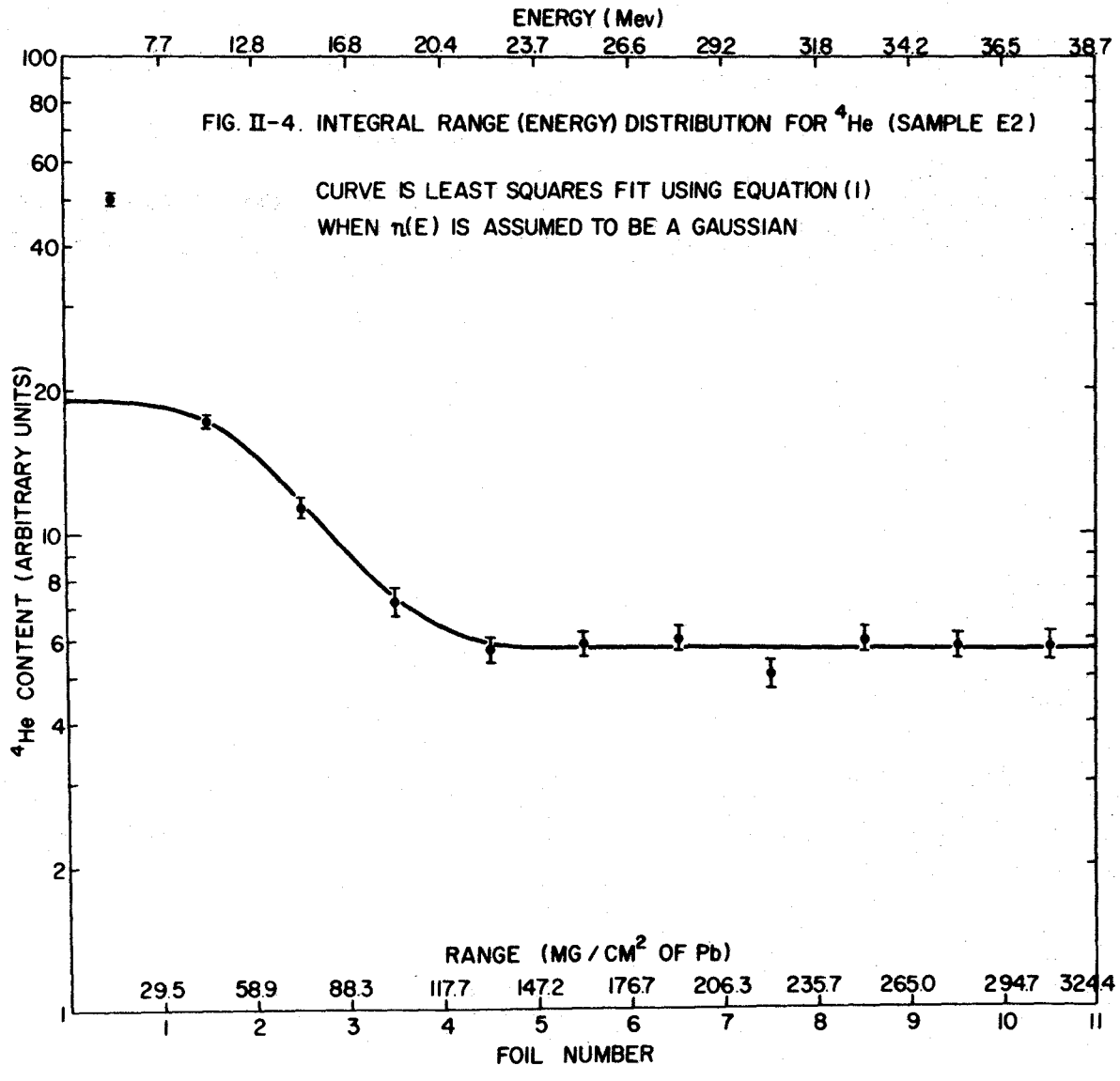

FIG. II-4. INTEGRAL RANGE (ENERGY) DISTRIBUTION FOR ^{4}He (SAMPLE E2)

CURVE IS LEAST SQUARES FIT USING EQUATION (1)
WHEN $\eta(E)$ IS ASSUMED TO BE A GAUSSIAN

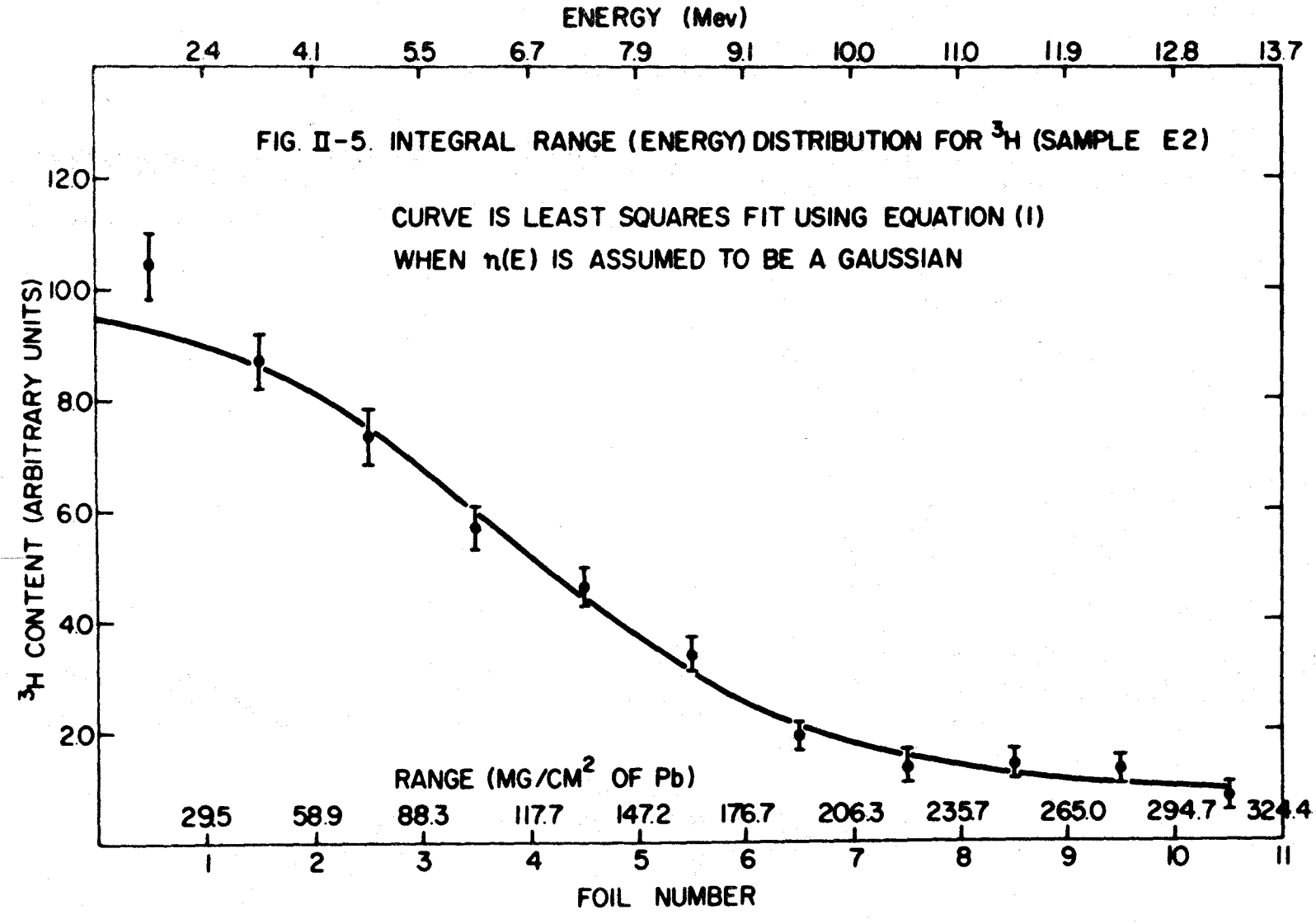
ENERGY (Mev)
2.4
4.1
5.5
6.7
7.9
9.1
10.0
11.0
11.9
12.8
13.7
FIG. II-5. INTEGRAL RANGE (ENERGY) DISTRIBUTION FOR ^3H (SAMPLE E2)
CURVE IS LEAST SQUARES FIT USING EQUATION (1)
WHEN n(E) IS ASSUMED TO BE A GAUSSIAN
^3H CONTENT (ARBITRARY UNITS)
120
100
80
60
40
20
RANGE (MG/CM^2 OF Pb)
29.5
58.9
88.3
117.7
147.2
176.7
206.3
235.7
265.0
294.7
324.4
1
2
3
4
5
6
7
8
9
10
11
FOIL NUMBER

Earlier work on energy spectra of light charged particles from fission has shown that these distributions can be fitted adequately with a gaussian function. Accordingly, the integral range distributions of Figs. II-4 and II-5, when reduced to units of energy, should be fitted with the function (see equation (1)):

$$N_i = a_1 + a_2\left[\Delta t_i \int_{E(t_i)}^{\infty} \frac{\exp[-(E-a_3)^2/2\ a_4^2]}{r(E)}\, dE + \right.$$

$$\left. + \int_{E(t_{i-1})}^{E(t_i)} \frac{(r(E)-t_{i-1})}{r(E)} \exp[-(E-a_3)^2/2\ a_4^2]\, dE \right]$$

The solid line shown in Figs. II-4 and II-5 is a least squares fit to the data when the first point is omitted in each case. The first point of the ^{4}He spectrum reflects an obvious departure from the assumed gaussian distribution and is evidence for a short-range component. The ^{3}H spectrum, also, suggests the presence of a short-range component, although less convincingly. Differential energy distributions obtained for ^{4}He and ^{3}H (sample E2) are shown in Figs. II-6 and II-7, respectively. Values obtained from the parameters of the fitted curves

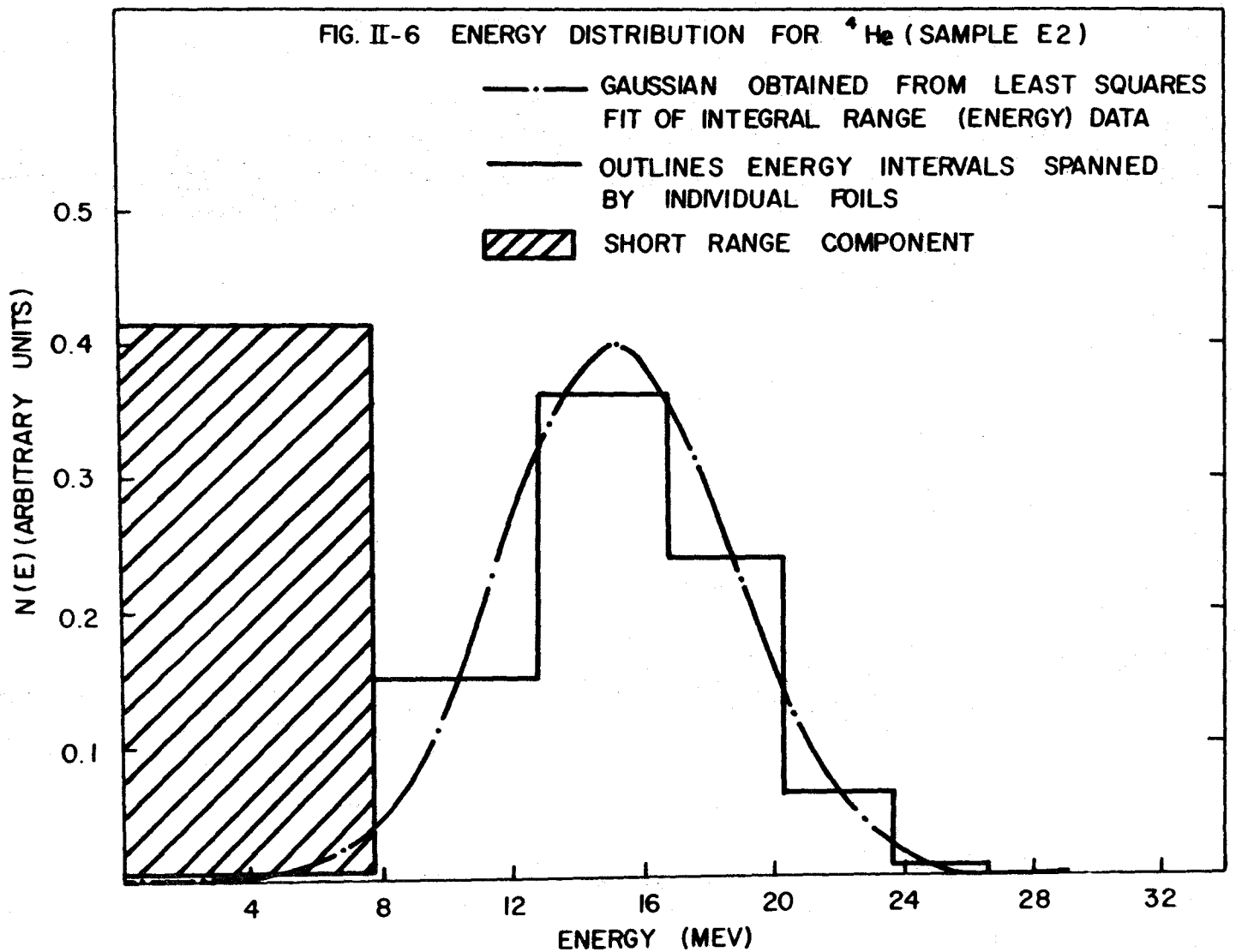
FIG. II-6 ENERGY DISTRIBUTION FOR ^{4}He (SAMPLE E2)
GAUSSIAN OBTAINED FROM LEAST SQUARES FIT OF INTEGRAL RANGE (ENERGY) DATA
OUTLINES ENERGY INTERVALS SPANNED BY INDIVIDUAL FOILS
SHORT RANGE COMPONENT
N(E) (ARBITRARY UNITS)
0.5
0.4
0.3
0.2
0.1
4
8
12
16
20
24
28
32
ENERGY (MEV)

FIG. II-7 ENERGY DISTRIBUTION FOR ^{3}H (SAMPLE E2)

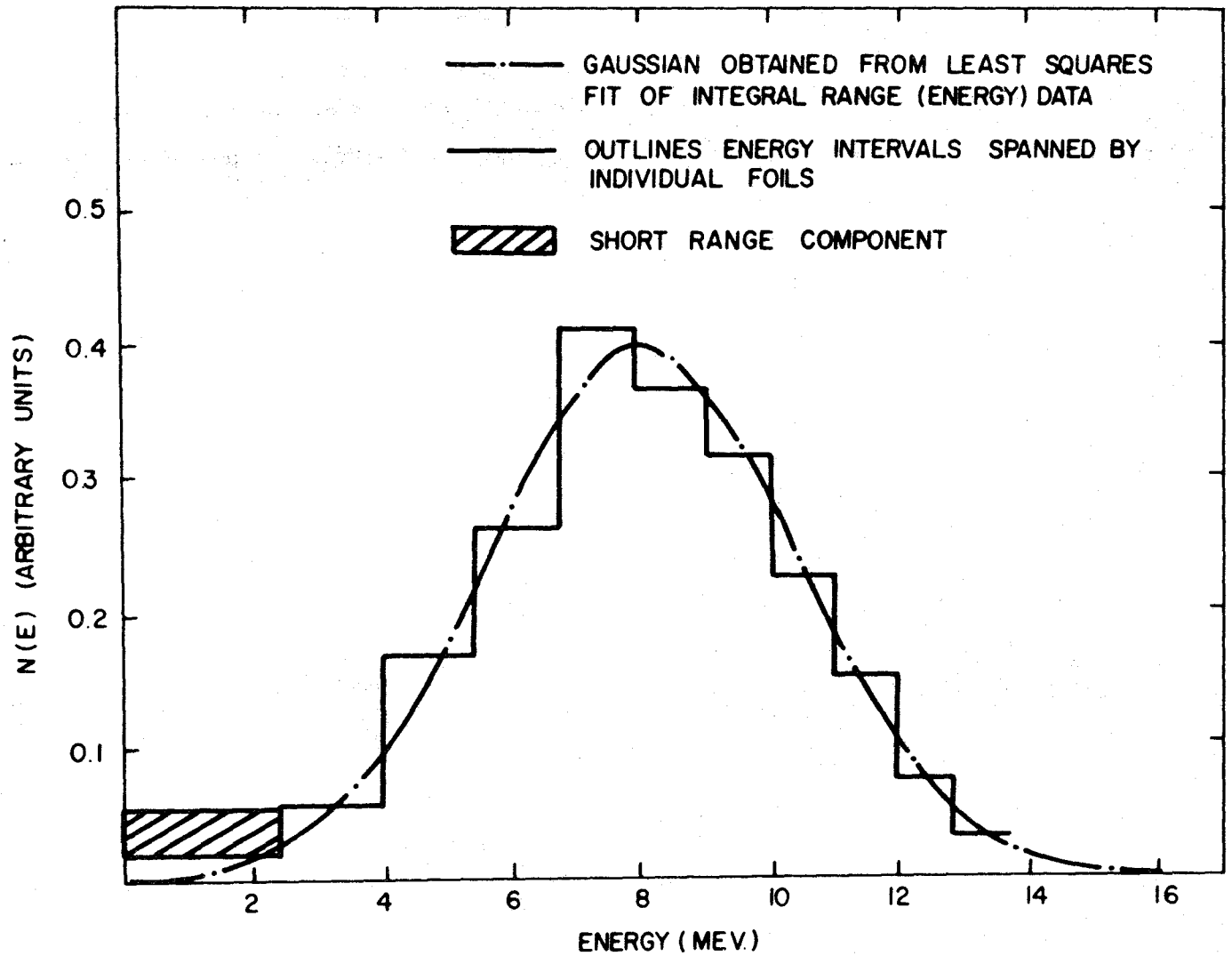

for most probable energy and width of the gaussian distributions are listed in Table II-5. Also given are the relative amounts of long-range and short-range components of ^4He and ^3H.

In part A of this chapter the ratios $^3H/^4He$ and $^3He/^4He$, as well as the absolute frequency of formation of ^4He were established. These values can now be broken down into long-range and short-range components. Using the relative amounts indicated in Table II-5, the following values are obtained:-

(a) Long-range particles:

$$^3H/^4He = (3.1 \pm 0.8) \times 10^{-2}$$
$$^3He/^4He = (2\ ^{+\ 6}_{-\ 2}) \times 10^{-6}$$
$$^4He/BF = (2.18 \pm 0.11) \times 10^{-3}$$
$$= 1\ ^4He \text{ atom in } 459 \pm 22 \text{ fissions.}$$

(b) Short-range particles:

$$^3H/^4He = (1 \pm 0.6) \times 10^{-3} \text{ (assuming short-range } ^3H \text{ formation)}$$
$$^3He/^4He = (7 \pm 4) \times 10^{-6} \text{ (assuming short-range } ^3He \text{ formation)}$$
$$^4He/BF = (2.09 \pm 0.10) \times 10^{-3}$$
$$= 1\ ^4He \text{ atom in } 478 \pm 24 \text{ fissions.}$$

Table II-5

Results of energy distribution measurements

Sample	MPE* (Mev)		FWHM** (Mev)		LRC/SRC***	
	^4He	^3H	^4He	^3H	^4He	$^3H(^3He)$
E1	15.4 ± 0.5		10.3 ± 0.9		1.06 ± 0.06	
E2	15.2 ± 0.4	8.0 ± 0.2	8.4 ± 0.9	5.5 ± 0.6	1.02 ± 0.06	(30 ± 15)
E3	15.4 ± 0.2		10.2 ± 0.6			
mean	15.4 ± 0.2	8.0 ± 0.2	9.8 ± 0.4	5.5 ± 0.6	1.04 ± 0.4	(30 ± 15)

*MPE = Most Probable Energy

**FWHM = Full Width at Half Maximum

***LRC/SRC = Long-Range Component/Short-Range Component. The short-range component in the ^3H energy spectrum may be due to short-range ^3He. No measurement of short-range $^3He/^4He$ as a function of cooling period was made.

IV

DISCUSSION

A. ORIGIN OF SHORT-RANGE PARTICLES

(i) Neutron reactions.

Possible contributions to short-range ^{4}He particles due to (n, α) reactions on targets, other than ^{235}U, in the fission source and Pb foils have been ruled out by the results of the control experiments discussed in the last chapter. The reaction $^{235}U(n_{th},\alpha)^{232}Th$ remains to be considered.

From the observed absolute yield of short-range ^{4}He particles, and known fission cross-sections of ^{235}U, it is easily calculated that the reaction $^{235}U(n_{th},\alpha)^{232}Th$ would require a cross-section of 1.2 barn (1 barn = $10^{-24}cm^{2}$) to produce these amounts of He. Total cross-sections for this reaction have not been measured but Chwaszczewska *et al*. (62) have been able to set upper limits of 3 mb and 2 mb for the transitions to the ground state and to any excited state of ^{232}Th up to 5 Mev, respectively (general trends of (n,α) cross-sections for the very heavy elements produce order of magnitude

estimates which are <1 μb). It therefore seems highly improbable that the observed ^{4}He is due to (n, α) reactions.

Information on cross-sections for the $^{235}U(n, t)^{233}Pa$ and $^{235}U(n, ^{3}He)^{233}Th$ reactions is lacking, and it is therefore not possible to rule out these reactions as sources for the short-range ^{3}He observed.

(ii) Heavy ion reactions.

Compound nucleus formation involving binary fission fragments and nuclei such as oxygen or nitrogen, with subsequent evaporation of alpha particles, must be considered as a potential source for short-range ^{4}He particles.

Assuming the fission source to consist entirely of U_3O_8 (the presence of appreciable amounts of C or N in the source will not affect the following argument), and knowing the flux of binary fission fragments, the reaction cross-section required to produce the observed ^{4}He is calculated to be 75 b (estimated accuracy of ±20%). Typical total reaction cross sections for 100 and 150 Mev ^{12}C and ^{16}O projectiles, respectively, on targets in the mass region spanned by the binary fission fragments are ~2 b (63). The most prominent mode of de-excitation in such reactions is multiple neutron evaporation. Cross-

sections for reactions leading to alpha emission are normally a small fraction of the total. Representative are values of ~200 mb for alpha emission from the system $^{140}Ce + {}^{16}O$ (90 Mev) (63). For the slightly lower average energies of binary fission fragments still lower cross-sections obtain. Clearly, heavy ion reactions induced by fission fragments could account for at most a fraction of one per cent of observed ^{4}He.

(iii) Scattering of atmospheric helium.

Atmospheric He atoms in the space between fission source and first Pb foil may be scattered by fission fragments and become embedded in the first foil. To determine the magnitude of this contribution to the observed short-range ^{4}He an analysis based on Rutherford scattering and trapping probabilities of low energy He atoms in Pb was carried out (see Appendix B).

In Appendix B it is shown that scattering phenomena can account for <0.1% of ^{4}He observed in the first foil. An upper limit is obtained since Coulomb screening effects for the scattered nuclei were neglected. These may be quite large for the mostly small angle (large impact parameter) scattering events considered.

Supporting evidence for the absence of appreciable contributions from scattering events is derived from an independent experimental study of Kr and Xe fission yields of ^{252}Cf carried out in this laboratory. Al foil (5.5 mg/cm^2) was suspended about 2 mm above a ^{252}Cf source (strength ~10^6 fissions/min) deposited on stainless steel backing. Fission fragments recoiled into the Al foil after traversing at least 2 mm of air, and were later analyzed for relative amounts of Kr and Xe isotopes present. Due to scattering of atmospheric Kr atoms by fission fragments in the space between source and foil, a component of atmospheric Kr would be expected in addition to fission product Kr in the foil. Assuming roughly equal "collection efficiencies" for Kr and He (determined by product of scattering cross-section and trapping probability) a ratio of $^{86}Kr_{atm.}/^{86}Kr_{fission} = 0.8$ is expected, if it is also assumed that all short-range ^4He in the ^{235}U experiment is due to scattering events. Measured $^{86}Kr_{atm.}/^{86}Kr_{fission}$ for one foil was 0.011, and it is considered that the small observed atmospheric Kr component was more probably due to other effects, such as memory in the mass spectrometer or blank foil Kr content.

Based on these considerations it is considered highly unlikely that a measurable amount of short-range ^4He extracted from the Pb catcher foil adjacent to the

^{235}U source was due to scattered atmospheric He.

(iv) Fission.

The present experiments indicate that the observed short-range ^{4}He particles are produced in the fission act itself (short-range ^{3}H or ^{3}He may also be produced, but the evidence is less certain). Early experiments using nuclear emulsions and coincidence techniques (see introduction) had indicated that short-range particles were produced with a frequency of about one in every hundred fissions of ^{235}U. No positive identification of the emitted light isotopes was obtained in those studies. The energy of the short-range particles was estimated to be about 1 Mev, and emission was observed to be mostly at right angles to the direction of the heavy fragments (52).

In this work it has been established that short-range ($E < 7.7$ Mev) ^{4}He particles are emitted in thermal neutron fission of ^{235}U with a frequency of one in 478 ± 24 fissions. Energetically, emission of ^{4}He nuclei must be favoured over any other light particle (except neutrons) and it is unlikely that the total number of other possible short-range particles emitted would amount to 1% of the total number of fissions. Results of the early experiments

may have included events other than ternary fissions.

It may be assumed that at least some of the events seen in the early experiments were short-range ^{4}He particles emitted at the instant of scission. Accepting the results of measurements of energy and angle of emission obtained using nuclear emulsions, it must be concluded that these short-range ^{4}He particles, as well as the long-range particles, are released in the region between two heavy fragments. In order to escape this region of relatively high coulomb potential energy with as little as 1 Mev of kinetic energy the particles must be released only in cases of extreme deformation of the heavy fragments, and at a very late stage of the scission act, such that unusually large distances between the centres of the heavy fragment nuclei and the alpha particle obtain at this instant.

It is difficult to postulate a mechanism for the emission of low-energy particles in fission based on the limited information available. Some correlation between required release energy and emission probability for a particular particle is expected. In addition, a "cluster probability" may be a determining factor in this process, since it is necessary at some stage of the fission act to transfer the required release energy to an appropriate assembly of nucleons.

B. LONG-RANGE PARTICLES

(i) Energy distributions

Measurement of the energy distributions for ^{3}H and ^{4}He produced in fission were originally intended to give information on the short-range components already discussed. Apart from revealing the presence of these low-energy particles however, these measurements are the first to be carried out using the present techniques. The results obtained are therefore independent confirmation of earlier, entirely different experiments on energy distributions of long-range ^{3}H and ^{4}He. Table II-6 summarizes recent published data for ^{3}H and ^{4}He from ^{235}U, ^{252}Cf, ^{233}U, and ^{239}Pu fission.

The values obtained in this work for most probable energies and widths of distributions are in excellent agreement with other published values of these parameters. Also listed in Table II-6 is the observed energy interval in each experiment. The present work did not have a low-energy cut-off and made possible detection of the short-range components. All other experiments listed in Table II-6 employed counter telescopes and were unable to observe the low-energy portion of the spectrum.

Table II-6

Parameters of energy distributions for long-range ^{4}He and ^{3}H produced in fission

Fissioning Nucleus	^{4}He MPE* (Mev)	^{4}He FWHM** (Mev)	^{4}He Observed Interval (Mev)	^{3}H MPE* (Mev)	^{3}H FWHM** (Mev)	^{3}H Observed Interval (Mev)
^{235}U ***	15.4 ± 0.2	9.8 ± 0.4	0 -26	8.0 ± 0.2	5.5 ± 0.6	0 -14
^{235}U (62)	16.2 ± 0.5	12 ± 1	5 -17.5	- - - - -	- - - - -	- - - -
^{235}U (64)	15.7 ± 0.3	9.8 ± 0.4	12 -32	8.6 ± 0.3	6.7 ± 0.6	6 -17
^{252}Cf(40)	15	(11)	10 -30	- - - - -	- - - - -	- - - -
^{252}Cf(49)	16.0 ± 0.2	(10.2 ± 0.4)	8.3-37.7	8.0 ± 0.3	(6.2 ± 0.6)	6.5-24.3
^{252}Cf(48)	16 ± 0.5	11.5 ± 0.5	7.8-34.8	8 ± 1	6 ± 1	3.9-23.1
^{233}U (50)	15.6	9.4	12.8-26.7	7.0	3	5.3-11.1
^{239}Pu(65)	16.0 ± 0.1	10.6 ± 0.2	10 -29	8.2 ± 0.2	7.6 ± 0.4	5.5-20

*MPE = Most Probable Energy

**FWHM = Full Width at Half Maximum. Parentheses indicate measurement of Half Width only

***Results obtained in this work

The energy distributions of ^{4}He and ^{3}H emitted in fission are seen to differ very little for different fissioning systems. Also, the MPE (most probable energy) for ^{3}H is seen to be roughly one half that for ^{4}He in each case. This behaviour is expected when one assumes that all light charged particles are emitted in the space between two heavy fragments at the instant of fission. Mutual Coulomb repulsion will endow the particles with the major portion of their final kinetic energies. Average nuclear charges for heavy fragments of the different fissioning nuclides do not vary greatly and should therefore produce nearly the same MPE for a particular light particle. Also, ^{3}H having half the nuclear charge of ^{4}He will attain only half the kinetic energy of ^{4}He. Both these predictions are borne out by the results of this work and those of other experiments.

(ii) Probability of emission of long-range ^{4}He in fission of ^{235}U.

The absolute frequency of formation of long-range alpha particles in fission has been measured by a variety of techniques, but results obtained are in generally poor agreement. Table II-7 summarizes published data on long-range ^{4}He from slow-neutron fission of ^{235}U.

TABLE II-7

Probability of emission of long-range ^{4}He in slow-neutron fission of ^{235}U

Reference	Experimental Technique	# atoms ^{4}He to # fissions
This work	mass spectrometry	1:459 ± 22
(43)	nuclear emulsions	1:230 ± 26
(52)	nuclear emulsions	1:340 ± 40
(54)*	nuclear emulsions	1:401 ± 50
(69)	nuclear emulsions	1:333 ± 111
(44)	ionization chambers in coincidence	1:505 ± 50
(67)	ionization chamber	1:220 ± 33
(71)	ionization chambers in coincidence	1:250
(45)	Cs I scintillator	1:449 ± 30
(70)	Cs I scintillator with magnetic spectrograph	1:310
(66)**	solid state detectors	1:518 ± 13
(68)*	solid state detectors	1:594 ± 65

* Values shown are corrected values given in Table V of reference (72).

** Indicated value is one of three measurements in reference (66), the other two values being: 1:512 ± 14 and 1:490 ± 20

It can be seen that values given vary by more than a factor of 2.5. A rough correlation appears to exist between experimental technique used and emission probability obtained. Nuclear emulsion and ionization chamber measurements show generally higher probabilities than the two values obtained using solid state detectors. A small variation can be accounted for by the fact that some experiments detected all long-range particles (including several per cent contribution from ^{3}H, and other particles), whereas other studies measured alpha particle emission only.

An additional factor, uncovered by the present experiments, may be the inclusion of varying proportions of short-range ^{4}He particles in some experiments, but not in others. Nuclear emulsions and some ionization chamber studies may register events attributable to short-range particles, whereas solid state detectors do not observe these due to some imposed low-energy cut-off. It is to be noted that short-range plus long-range ^{4}He observed in the present work yield a total ^{4}He emission probability of 1:234. All values, except the two obtained using solid state detectors, lie between the limits 1:234 and $1:459 \pm 22$, representing total ^{4}He and long-range ^{4}He, respectively, measured in this work.

The mass spectrometric techniques used in this study are considered more reliable than others for measurement of emission probability of long-range ^{4}He. This method eliminates spurious events by achieving unambiguous particle identification and attains necessary resolution from short-range particles.

Due to the rather large variations in results obtained to date it has been difficult to determine any dependence of emission probabilities for light particles as a function of the different parameters in different fission systems. Thomas and Whetstone (72) have nevertheless indicated a variation between emission probability and excitation energy of initial compound nucleus. Values decrease from about 1:300 for zero excitation (^{252}Cf fission) to about 1:500 for 6.5 Mev excitation ($^{235}U + n_{th}$), and increase again at higher excitation energies. Nobles (45), on the other hand, has been able to show an increasing probability of emission with increasing Z^2/A of the fissioning nucleus. Further accurate measurements of emission probabilities for light charged particles in fission will be required before an adequate explanation of these phenomena can be given.

(iii) Relative yields of ^{3}H, ^{3}He, and ^{4}He in fission of ^{235}U.

Relative yields of the various light particles emitted in ternary fission may ultimately provide a sensitive test for any theory attempting to explain this process. According to Halpern (46) it does not seem possible to explain the relative yields on the basis of conventional evaporation theory. Such an approach could not account for the observed angular distribution in a simple way (one would expect isotropic emission), and would predict unreasonably high neutron/light charged particle ratios. Generally, one expects some inverse correlation between particle yield and release energy required, but lack of accurate experimental data has not permitted determination of the exact functional dependence.

In Table II-8 some recent, published relative yields for ^{3}H, ^{3}He, and ^{4}He are listed for several different fissioning species. A discrepancy exists between the values for $^{3}H/^{4}He$ found in this work and that of Dakowski et al. (64). Differences in values for $^{3}H/^{4}He$ between different fission systems may be real or again be partly due to the different experimental techniques employed. The present technique is considered more reliable primarily since particle identification is unambiguous,

Table II-8

Relative yields for ^{3}H, ^{3}He, and ^{4}He in fission

Fissioning Nucleus	Reference	$\frac{^{3}H}{^{4}He}$	$\frac{^{3}He}{^{4}He}$
^{235}U	This work	$(3.1 \pm 0.8) \times 10^{-2}$	$(2^{+6}_{-2}) \times 10^{-6}$
^{235}U	(64)	$(6.2 \pm 0.5) \times 10^{-2}$	
^{233}U	(50)	2.8×10^{-2}	$\simeq 1.8 \times 10^{-2}$
^{239}Pu	(65)	$(6.8 \pm 0.3) \times 10^{-2}$	
^{252}Cf	(48)	$(5.9 \pm 0.2) \times 10^{-2}$	$\lesssim 9 \times 10^{-3}$
^{252}Cf	(49)	$(8.46 \pm 0.28) \times 10^{-2}$	$\leq 7.5 \times 10^{-4}$

whereas experiments using counter telescopes achieve less positive resolution between the numerous events observed. Existing data therefore can not illuminate any significant differences, should they exist, between relative yields of ^{3}H and ^{4}He for the different fissioning nuclides.

Cambiaghi et al. (50) claim positive observation of ^{3}He emitted in fission of ^{233}U. Their measured yield is in sharp contrast to the value obtained in this work for ^{235}U, as well as the upper limits reported for ^{252}Cf. Cambiaghi et al. consider the differences between their value and those for ^{252}Cf significant. They suggest, therefore, that the functional dependence of the form

$$\text{yield} \propto \exp(-E_R/T),$$

where E_R is the release energy and T a nuclear temperature (suggested by Whetstone and Thomas for ^{252}Cf fission (48)) may not be applicable for all fission systems. The extremely low (possibly zero) yield for ^{3}He obtained in the present work for ^{235}U seems to cast doubt on the validity of some of the other measured ^{3}He yields. Even those events definitely ascribed to ^{3}He in ^{252}Cf fission may be spurious. Alternatively, if the large differences for $^{3}He/^{4}He$ suggested by existing data are verified in future experiments, they may provide a very sensitive test for any comprehensive theory of fission.

To conclude, the present study of ternary fission of ^{235}U has achieved the following:-

1) Upper limits for the yields of all stable and some radioactive isotopes of Ne and Ar have been established.
2) Short-range ^{4}He particles have been identified as fission products of ^{235}U.
3) Energy distributions for ^{4}He and ^{3}H produced in fission of ^{235}U were measured for the first time using mass-spectrometric techniques.
4) Relative yields for ^{3}H, ^{3}He, and ^{4}He were measured. The upper limit for direct ^{3}He formation, relative to ^{4}He, was determined to be: $^{3}He/^{4}He < 8 \times 10^{-6}$. This corresponds to less than one ^{3}He atom formed in 6×10^{7} fissions.

APPENDIX A

NUMBER OF PARTICLES FOUND IN A PARTICULAR FOIL OF A STACK COVERING A SOURCE OF FINITE AREA EMITTING PARTICLES ISOTROPICALLY

The geometrical arrangement of fission source and foil stack is shown schematically below:

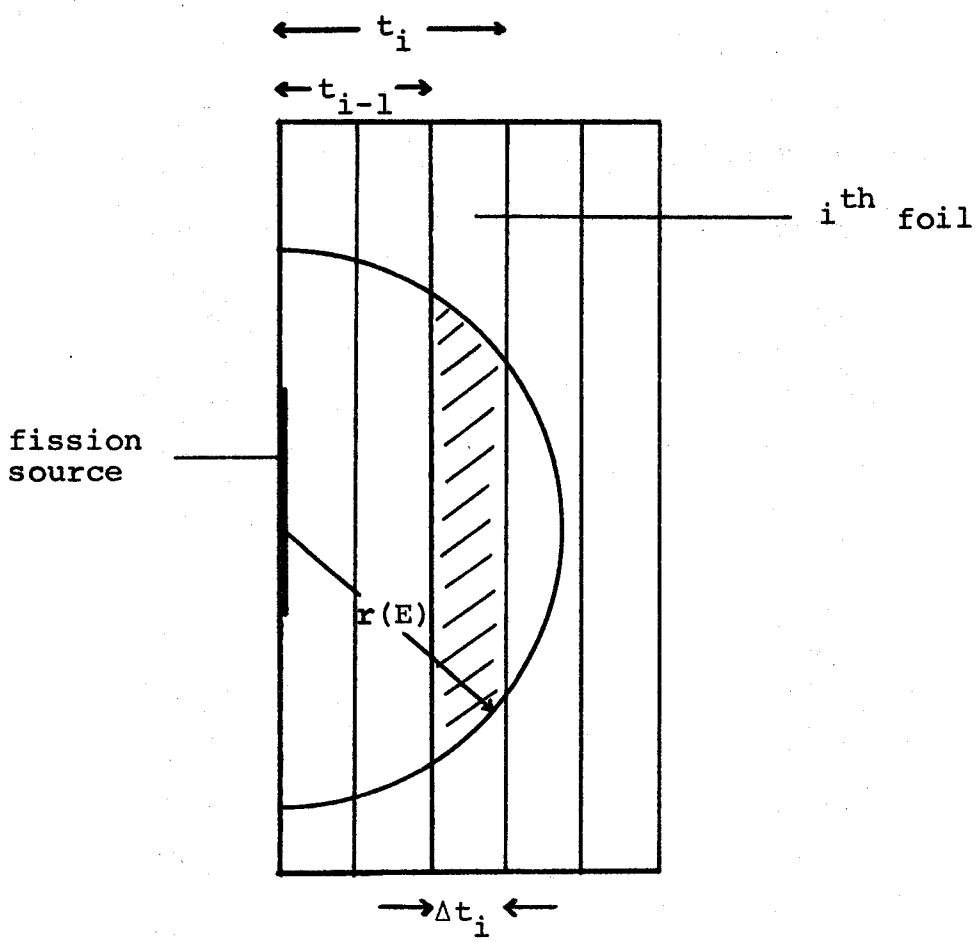

Assume particles are emitted isotropically and dimensions of the foil stack are such that all particles are stopped in the foil stack.

Let a particle be emitted in an arbitrary direction with range r(E) (E = energy), and be stopped in the i^{th} foil (see diagram). The probability of finding this particle in the i^{th} foil is equal to the ratio of the area of the shaded zone to the total surface area of the hemisphere of radius r(E), that is

$$p_i = \frac{2\pi\, r(E)\, \Delta t_i}{2\pi (r(E))^2}$$

$$= \frac{\Delta t_i}{r(E)}$$

This relation holds whenever $r(E) \geq t_i$. Obviously $p_i = 0$ when $r(E) \leq t_{i-1}$. For the case $t_{i-1} < r(E) < t_i$ one obtains

$$p_i = \frac{2\pi\, r(E)\, (r(E)-t_{i-1})}{2\pi (r(E))^2}$$

$$= \frac{r(E)-t_{i-1}}{r(E)}$$

The relations may be summarized as follows:

$$p_i = \frac{\Delta t_i}{r(E)} \qquad r(E) \geq t_i$$

$$= \frac{r(E)-t_{i-1}}{r(E)} \qquad t_{i-1} < r(E) < t_i$$

$$= 0 \qquad r(E) \leq t_{i-1}$$

Let a particle within energy interval dE around E be emitted with probability n(E) dE. The probability of finding a particle emitted with this energy in the i^{th} foil is then

$$P_i = p_i \times n(E)\ dE$$

The total probability of finding a particle in the i^{th} foil is therefore

$$\int_{E=0}^{E=\infty} P_i dE = \int_{E=0}^{E=\infty} p_i\ n(E)\ dE$$

$$= \Delta t_i \int_{E(t_i)}^{\infty} \frac{n(E)\ dE}{r(E)} +$$

$$+ \int_{E(t_{i-1})}^{E(t_i)} \frac{(r(E) - t_{i-1})}{r(E)}\, n(E) dE,$$

where $E(t_i)$ is the energy of a particle with range t_i.

The total number of particles found in foil i will be:

$$N_i = a_1 + a_2 \left\{ \Delta t_i \int_{E(t_i)}^{\infty} \frac{n(E)\,dE}{r(E)} + \int_{E(t_{i-1})}^{E(t_i)} \frac{(r(E)-t_{i-1})}{r(E)}\, n(E)\,dE \right\}$$

where a_1 = constant background

a_2 = constant depending on source strength

N_i was obtained experimentally. Least squares fits to the data points using the above equation, with $n(E)$ assumed to be a gaussian function, were obtained by means of numerical computations carried out on a digital computer.

APPENDIX B

ELASTIC SCATTERING OF ATMOSPHERIC HELIUM ATOMS BY FISSION FRAGMENTS

A scattering event between a moving fission fragment and a stationary He atom can be represented schematically as shown:

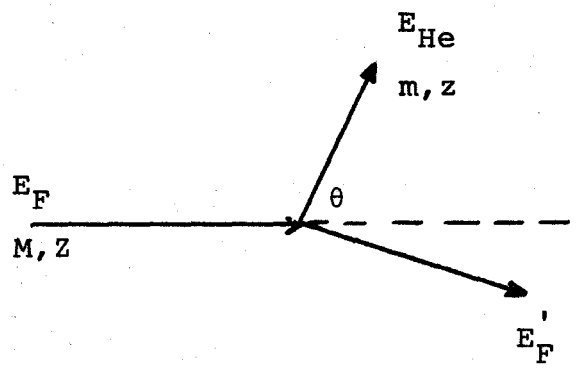

E_F, M, Z, and E_{He}, m, z are the energy, mass, and nuclear charge of the incident fission fragment and scattered He atom, respectively.

Neglecting screening effects the Rutherford cross-section for scattering a He atom at an angle θ or less (laboratory co-ordinates) is given by

$$\sigma(\leq\theta) = \pi P^2$$

where $$P = \frac{|Zz|e^2(m+M)}{2mE_F} \tan\theta \qquad \text{(B1)}$$

From conservation of energy and momentum it is readily found that:

$$\cos^2\theta = \frac{E_{He}(m+M)^2}{4mME_F} \qquad \text{(B2)}$$

It can be seen from equation (B1) that $\sigma(\leq\theta)\rightarrow\infty$ as $\theta\rightarrow\pi/2$. However, from equation (B2) one has $E_{He}\rightarrow 0$ as $\theta\rightarrow\pi/2$.

In principle, therefore, all He atoms present as target atoms will be scattered if arbitrarily low energies are considered. However, to trap a He atom permanently in a metallic foil it must have energy $E>E_{th}$, where E_{th} is the threshold for trapping to occur.

E_{th} for He in Pb may be estimated using the experimental data of Kornelson (73) in conjunction with the numerical values of interaction potentials between inert gas atoms reported by Abrahamson (74). E_{th} for He in tungsten is estimated to be ~8 ev, at which energy the trapping probability may be considered $<10^{-5}$. This probability rises sharply to ~0.5 at 100 ev and levels off slightly above this value in the kev energy region. Similar behaviour is expected for He trapping probabilities in Pb.

Alternatively, the minimum energy required by an ion or neutral atom to become permanently embedded in a target may be taken as the displacement energy E_d (the energy required to knock an atom out of its position in the lattice). E_d for Ge and Cu have been reported equal to 30 and 25 ev, respectively (75). E_d for Pb is expected to be comparable to these values.

The assumptions made with respect to the present calculations of He trapping in Pb are that the trapping probability is $<10^{-4}$ for $E_{He} \leq 10$ ev, and unity for $E_{He} > 100$ ev. These values are considered upper limits, although an error of one order of magnitude in either direction would not affect the present argument.

In calculating the Rutherford scattering cross-section the following values were considered typical for fission fragments: E_F = 80 Mev, M = 118 amu, Z = 46. Listed below are results of calculations of scattering cross-sections as well as estimated trapping probabilities of He at various energies:

E_{He} (ev)	σ (cm^2)	P_t	$\sigma \times P_t$ (cm^2)
10^6	1.8×10^{-22}	1.0	1.8×10^{-22}
10^5	2.0×10^{-21}	1.0	2.0×10^{-21}
10^4	2.0×10^{-20}	1.0	2.0×10^{-20}
10^3	2.0×10^{-19}	1.0	2.0×10^{-19}
10^2	2.0×10^{-18}	1.0	2.0×10^{-18}
10	2.1×10^{-17}	$<10^{-4}$	$<2.1 \times 10^{-21}$
1	2.3×10^{-16}	$(<10^{-8})$	$(<2.3 \times 10^{-24})$

The number of He atoms scattered by fission fragments and trapped by Pb foil is given by

$$He_{scatt.} = N \sigma \phi P_t T$$

where N = number of target He atoms

σ = scattering cross-section

ϕ = flux of fission fragments

P_t = trapping probability

T = period of irradiation

N was calculated by assuming a layer of air 0.1 mm thick at atmospheric pressure between fission source and Pb foil.

ϕ was determined from the number of fissions and period of irradiation.

The ratio of scattered atmospheric He expected, to short-range fission He found in the Pb foil adjacent to the fission source, was calculated for various energies E_{He} and is shown below:

E_{He} (ev)	$\frac{He\ scatt.}{He\ fission}$
10^6	1.2×10^{-7}
10^5	1.4×10^{-6}
10^4	1.4×10^{-5}
10^3	1.4×10^{-4}
10^2	1.4×10^{-3}
10	$<1.5 \times 10^{-6}$
1	$(<1.6 \times 10^{-9})$

It can be seen that the ratio of atmospheric to fission He expected is at most $\sim 10^{-3}$. Therefore the observed short-range He particles can not contain a measurable contribution due to scattered atmospheric helium.

BIBLIOGRAPHY

1. Hahn, O., and Strassmann, F., Naturwiss. 27, 11, 89 (1939).
2. Bohr, N., and Wheeler, J., Phys. Rev. 56, 426 (1939).
3. Wheeler, J., as reported in: "Radiochemical Studies: The Fission Products", National Nuclear Energy Series, ed. C. D. Coryell and N. Sugarman (New York: McGraw-Hill Book Company, Inc., 1951); Book I, p. 343.
4. Present, R. D., and Knipp, J. K., Phys. Rev. 57, 751, 1188 (1940).
5. Present, R. D., Phys. Rev. 59, 466 (1941).
6. Metcalf, R. P., Seiler, J. A., Steinberg, E. P., and Winsberg, L., Radiochemical Studies: The Fission Products, National Nuclear Energy Series, ed. C. D. Coryell and N. Sugarman (New York: McGraw-Hill Book Company, Inc., 1951); papers 47-51.
7. Alvarez, L. W., as reported by Farwell, G., Segrè, E., and Wiegand, C., Phys. Rev. 71, 327 (1947).
8. Fleischer, R. L., Price, P. B., Walker, R. M., and Hubbard, E. L., Phys. Rev. 143, 943 (1966).

9. Karamyan, S. A., Kuznetsov, I. V., Oganeskyan, Yu. Ts., and Peniouzhkevich, Yu. E., Soviet J. Nucl. Phys. 5, 684 (1967).

10. Iyer, R. H., and Cobble, J. W., Phys. Rev. Lett. 17, 541 (1966).

11. Iyer, R. H., and Cobble, J. W., Phys. Rev. 172, 1186 (1968).

12. Hyde, E. K., The Nuclear Properties of the Heavy Elements, Vol. III (Prentice-Hall, Inc., Englewood Cliffs, New Jersey, 1964).

13. Perfilov, N. A., Physics of Nuclear Fission (Pergamon Press Ltd., London), Chap. 7, 84 (1958).

14. Titterton, E. W., Nature 168, 590 (1951).

15. Rosen, L., and Hudson, A. M., Phys. Rev. 78, 533 (1950).

16. Muga, M. L., Phys. Rev. Lett., 11, 129 (1963).

17. Muga, M. L., Physics and Chemistry of Fission (Proc. Symp. Salzburg, 1965) IAEA, Vienna, 1965.

18. Muga, M. L., Rice, C. R., and Sedlacek, W. A., Phys. Rev. Lett. 18, 404 (1967).

19. Muga, M. L., Rice, C. R., and Sedlacek, W. A., Phys. Rev. 161, 1266 (1967).

20. Muga, M. L., and Rice, C. R., Physcis and Chemistry of Fission (Proc. Symp. Vienna 1969) IAEA, Vienna, 1969.

21. Stoenner, R. W., and Hillman, M., Phys. Rev. 142, 716 (1966).

22. Prestwood, R. J., and Bayhurst, B. P., Bull. Am. Chem. Soc., Abstract J15 (1966).

23. Fleming, W. H., and Thode, H. G., Phys. Rev. 90, 857 (1953).

24. Wetherill, G. W., Phys. Rev. 96, 679 (1954).

25. Shukolyukov, Yu. A., Tolstikhin, I. N., and Ashkinadze, G. Sh., Geochem. Int. 3, 738 (1966).

26. Gerling, E. K., Shukolyukov, Yu. A., Tolstikhin, I. N., and Ashkinadze, G. Sh., Geochem. Int. 3, 1140 (1966).

27. Farrar, H., and Tomlinson, R. H., Nucl. Phys. 34, 367 (1962).

28. Eberhardt, P., Eugster, O., and Marti, K., Z. Naturf. 20A, 623 (1965).

29. Nier, A. O., Phys. Rev. 79, 450 (1950).

30. Roy, J. C., Can. J. Phys. 39, 315 (1961).

31. Steinberg, E. P., Wilkins, B. D., Kaufman, S. B., and Fluss, J. M., Phys. Rev. C 1, No. 6, 2046 (1970).

32. Natowitz, J. B., Khodai-Joopari, A., and Alexander, J. M., Phys. Rev. 169, 993 (1968).

33. For detailed references to early studies see: "The Nuclear Properties of the Heavy Elements, Vol. III", ed. E. K. Hyde (Prentice-Hall Inc., Englewood Cliffs, New Jersey, 1964).

34. Tsien San Tsiang, J. Phys. Radium 9, 6 (1948).

35. Hill, D. L., Phys. Rev. 87, 1049 (1952).

36. Albenesius, E. L., Phys. Rev. Lett. 3, 274 (1959).

37. Feather, N., Physics and Chemistry of Fission (Proc. Symp. Vienna, 1969) IAEA, Vienna, 1969.

38. Gazit, Y., Nardi, E., and Katcoff, S., Phys. Rev. C 1, No. 6, 2101 (1970).

39. Raisbeck, G. M., and Thomas, T. D., Phys. Rev. 172, 1272 (1968).

40. Fraenkel, Z., Phys. Rev. 156, 1283 (1967).

41. Boneh, Y., Fraenkel, Z., and Nebenzahl, I., Phys. Rev. 156, 1305 (1967).

42. Blocki, J., and Krogulski, T., Nucl. Phys. A122, 417 (1968).

43. Marshall, L., Phys. Rev. 75, 1339 (1949).

44. Allen, K. W., and Dewan, J. T., Phys. Rev. 80, 181 (1950).

45. Nobles, R. A., Phys. Rev. 126, 1508 (1962).

46. Halpern, I., Physics and Chemistry of Fission (Proc. Symp. Salzburg, 1965) IAEA, Vienna, 1965.

47. Feather, N., Proc. Roy. Soc. (Edinburgh) A68, 229 (1969).

48. Whetstone, S. L., and Thomas, T. D., Phys. Rev. 154, 1174 (1967).

49. Cosper, S. W., Cerny, J., and Gatti, R. C., Phys. Rev. 154, 1193 (1967).

50. Cambiaghi, M., Fossati, F., and Pinelli, T., Nuovo Cim. 59B, 236 (1969).

51. Cassels, J. M., Dainty, J., Feather, N., and Green, L. L., Proc. Roy. Soc. (London) A191, 428 (1947).

52. Green, L. L., and Livesey, D. L., Trans. Roy. Soc. (London) A241, 323 (1948).

53. Tsien San Tsiang, Ho Zah-Wei, Chastel, R., and Vigneron, L., J. Phys. Radium, 8, 165, 200 (1947).

54. Titterton, E. W., Nature 168, 590 (1951).

55. Allen, K. W., and Dewan, J. T., Phys. Rev. 82, 527 (1951).

56. Muga, M. L., Bowman, H. R., and Thompson, S. G., Phys. Rev. 121, 270 (1961).

57. Handbook of Chemistry and Physics (The Chemical Rubber Co.) 49 Ed., 1968-1969.

58. Hoffman, J. H., letter to D. Lal, March, 1967.

59. Table of Isotopes, 6 Ed., ed. C. M. Lederer, J. M. Hollander, and I. Perlman (John Wiley and Sons Inc., New York, 1967).

60. Whaling, W., Handbuch der Physik, ed. S. Flügge (Springer-Verlag, Berlin, 1958) Vol. 34, 197 (1958).

61. Williamson, C. F., Boujot, J. P., and Picard, J., "Tables of Range and Stopping Power of Chemical Elements for Charged Particles of Energy 0.05 to 500 Mev", (Centre D'Études Nucléaires de Saclay) Rapport CEA-R3042, July, 1966.

62. Chwaszczewska, J., Dakowski, M., Krogulski, T., Piasecki, E., Sowiński, M., Stegner, A., and Tys, J., Acta Phys. Polon. 35, 187 (1969).

63. Thomas, T. D., Ann. Rev. Nucl. Sc. 18, 343 (1968).

64. Dakowski, M., Chwaszczewska, J., Krogulski, T., Piasecki, E., and Sowiński, M., Phys. Lett., 25B, No. 3, 213 (1967).

65. Krogulski, T., Chwaszczewska, J. Dakowski, M., Piasecki, E., Sowiński, M., and Tys, J., Nucl. Phys. A128, 219 (1969).

66. Schröder, I. G., Deruytter, A. J., and Moore, J. A., Phys. Rev. 137, B519 (1965).

67. Hill, D. L., Phys. Rev. 87, 1049 (1952).

68. Hattangadi, V. A., Methasiri, T., Nadkarni, D. M., Ramanna, R., and Rama Rao, P. N., Physics and Chemistry of Fission (Proc. Symp. Salzburg, 1965) IAEA, Vienna 1965.

69. Tsien San Tsiang, Ho Zah-Wei, Chastel, R., and Vigneron, L., Compt. Rend. 224, 272 (1947).

70. Fulmer, C. B., and Cohen, B. C., Phys. Rev. 108, 370 (1957).

71. Farwell, G., Segrè, E., and Wiegand, C., Phys. Rev. 71, 327 (1947).

72. Thomas, T. D., and Whetstone, S. L., Phys. Rev. 144, 1060 (1966).

73. Kornelsen, E. V., Can. J. Phys. 42, 364 (1964).

74. Abrahamson, A. A., Phys. Rev. 130, 693 (1963).

75. Dienes, G. J., Proc. Int. Conf. on Peaceful Uses of Atomic Energy (United Nations, 1956), Vol. 7, 634 (1956).

76. Douthett, E. M., and Templeton, D. H., Phys. Rev. 94, 128 (1954).